STRATIGRAPHY OF UPPER MIOCENE OOLITE-MICROBIALITE-CORALGAL REEF SEQUENCES OF THE TERMINAL CARBONATE COMPLEX: SOUTHEAST SPAIN

BY

Christopher Jeremy Lipinski

Submitted to the graduate degree program in Geology
and the Graduate Faculty of the University of Kansas
in partial fulfillment of the requirements for the degree of
Master of Sciences.

_____
Co-chairperson

Committee members _____
Co-chairperson

_____

Date defended: _____

The Thesis Committee for Christopher Jeremy Lipinski certifies
that this is the approved Version of the following thesis:

STRATIGRAPHY OF UPPER MIOCENE OOLITE-MICROBIALITE-CORALGAL REEF SEQUENCES OF THE TERMINAL CARBONATE COMPLEX: SOUTHEAST SPAIN

Committee:

_____
Co-chairperson

_____
Co-chairperson

_____

Date approved: _____

ABSTRACT

Christopher Jeremy Lipinski
Department of Geology, November 2009
The University of Kansas

This study documents the stratigraphic characterization of the Terminal Carbonate Complex (TCC) at two locations within the Cabo de Gata area of southeast Spain, La Molata and La Rellana/Ricardillo. The TCC is a distinctive upper Miocene (Messinian) unit consisting of oolite, microbialite (stromatolites and thrombolites), and coralgal reefs deposited in association with high-amplitude cyclic glacioeustacy and evaporitic drawdown of the Mediterranean. The studied locations are approximately 5 km apart and were at or below elevations of late Messinian sea level highstands. Data collected included geologic mapping, 44 measured stratigraphic sections, tracing geometries on photomosaics, petrophysical analysis of 399 core plugs, and petrographic analysis of 87 thin sections.

Four cyclic sequences record four relative rises and falls in sea level with amplitudes of 53.6-83.5 m. Sequences commonly have local basal stromatolites overlain by local thrombolite boundstone that is overlain by trough cross-bedded ooid grainstone, which grades upward to volcaniclastic-rich planar bedded ooid grainstone capped by fenestral ooid grainstone. At low elevations, the thrombolite boundstones are thicker and laterally more continuous than at higher elevations. Thrombolites that are stratigraphically high in sequences may be interbedded with trough cross-bedded ooid grainstone.

At intermediate substrate elevations, sequences have a build-and-fill architecture, characterized by a relief-building phase followed by a relief-filling phase, with the

relatively thin sequences draping paleotopography. Microbialites dominate deposition during the relative sea-level rises and build topographic relief. Oolites dominate deposition during the relative sea-level falls and fill topographic relief. Most of the deposition is during the relative sea-level falls. At higher substrate elevations, close to the highstand position, sequences thicken and yield internal stratigraphic character that is inconsistent with a build-and-fill model. Apparently, the build-and-fill model requires an intermediate substrate elevation and non-optimal carbonate productivity during rapid sea level change.

Overall, the sequences progressively show increasing diversity and more normal marine organisms, which may have been caused by decreasing aridity. Lithofacies of the La Molata area evidence more restricted conditions compared to the La Rellana/Ricardillo area lithofacies, likely resulting from La Molata deposits forming in a protected embayment.

TABLE OF CONTENTS

LIST OF FIGURES AND TABLES

ACKNOWLEDGEMENTS

I would like to first of all thank my two advisors, Dr. Bob Goldstein and Dr. Evan Franseen, for all their time, effort, and support that they so willingly expended on me. They provided invaluable guidance and teachings that will last my lifetime. I am grateful for the opportunity to study at the University of Kansas and contribute to the ongoing study in Spain. Thanks go to the exceptional KU professors for the vast knowledge they imparted to me, which allowed me to appreciate all areas of geology. A special thanks goes to Jason Rush of the Kansas Geological Survey for his help with Petrel™ and to Alan Byrnes for his help with the petrophysical analysis. Right from the beginning, the entire office staff and Ian Rowell were always available and provided phenomenal assistance. I could not have asked more of my time at KU.

I would also like to thank my undergraduate geology department at the University of Wisconsin-Oshkosh, and especially my advisory there, Dr .Dan Lehrmann, for I would not be here if it were not for them. Gerald Gutoski, formerly of New Berlin West, needs special thanks for his extraordinary way to motivate and his passion for geology. Academia lost someone special with his retirement, but his legacy continues with the generations of geologists he inspired.

Most of all I would like to thank my Gorgeous, Amanda Mozina, for her unwavering support, her patience, and her motivation that without, this would not have been possible. Mike and Joanne Lipinski raised four admirable gentlemen and I cannot thank them enough for everything they have done for me; I love you.

INTRODUCTION

The Cabo de Gata volcanic province of southeastern Spain has been the focus for numerous studies of upper Miocene heterozoan and photozoan (reef) carbonate systems (Dabrio et al., 1981; Goldstein and Franseen, 1995; Whitesell, 1995; Esteban, 1996; Esteban et al., 1996; Franseen and Goldstein, 1996; Martin et al., 1996; Franseen et al., 1997a; Franseen et al., 1997b; Brachert et al., 1998; Franseen et al., 1998; Brachert et al., 2001; Martin et al., 2003; Toomey, 2003; Dillett, 2004; Martin et al., 2004; Johnson et al., 2005; Dvoretsky, 2009). Most previous studies in the Cabo de Gata region have described general stratigraphic relationships or concentrated on the heterozoan and reef systems. In contrast, few studies have focused on the Terminal Carbonate Complex, a unit that forms the last record of Miocene basin-margin deposition.

In the 1970's, Esteban and collaborators defined the Terminal Carbonate Complex (TCC) as a distinctive upper Miocene unit distributed around the Mediterranean (Esteban et. al., 1979). In the study area, the TCC consists of four topography-draping sequences composed of oolite, microbialite (thrombolite and stromatolite), and minor coralgal reefs, deposited in association with high-amplitude cyclic glacioeustacy and evaporitic drawdown of the Mediterranean (Franseen et al., 1993; Goldstein and Franseen, 1995; Franseen et. al., 1996; Franseen et al., 1998).

A more detailed understanding of the TCC, utilizing the excellent 3-D exposures in the Cabo de Gata area, is warranted for several reasons. Oolites are important reservoirs for oil and gas throughout the world (Honda et. al., 1989; Marcal et. al., 1998; Al Suwaidi et. al., 2000; Bishop, 2000; Davies et. al., 2000; Al Saad and Sadooni, 2001

Llinas, 2002; 2003; Qi and Carr, 2003; Holail et. al., 2006). Microbialite reservoirs have been large producers in the past (Hitzman, 1996; Tucker, 1997; Mancini et al., 1998, 2004, 2008; Mancini and Parcell, 2001; Heydari and Baria, 2005; Buchheim, 2009) and have received renewed interest with recent discoveries in the Santos basin, offshore Brazil. Microbialite and oolite assemblages are commonly deposited together with complex facies geometries and distributions both in the ancient (Riding et al., 1991; Sami and James, 1994; Braga et al., 1995; Aurell and Badenas, 1997; Feldman and McKenzie, 1997; Mancini et al., 1998, 2004, 2008; Grotzinger et al., 2000; Mancini and Parcell, 2001; Adams et al., 2004, 2005; Batten et al., 2004; Heydari and Baria, 2005) and in the modern (Feldman and McKenzie, 1998; Reid et al., 2003; Planavsky and Ginsburg, 2009). Therefore, the TCC can provide a useful outcrop analog for better understanding similar reservoir systems.

Similar to the TCC, many other oolite and microbialite-oolite systems formed during times of high-amplitude rises and falls in sea level. As demonstrated by (Franseen et al., 1993; Franseen et al. 1997a; Franseen and Goldstein, 2004; Franseen and Goldstein, 2007) the TCC sequences have sequence-stratigraphic characteristics (i.e. stratal and sequence geometries, lithofacies distributions) that are at least partially dependent on the interaction between substrate paleotopography and relative sea-level history. Therefore, detailed studies will lead to a better understanding of the depositional controls on oolite-microbialite systems at differing substrate elevations as sea level rises and falls, and can aid in refining sequence stratigraphic models for such systems. Specifically, carbonate sequence stratigraphic models (Read, 1985; Handford and Loucks, 1993) make excellent predictions for facies expected in highstand and lowstand

positions. Sequence stratigraphic models have not been worked out effectively for intermediate substrate elevations, however. Franseen and Goldstein (2004) hypothesized that carbonate systems characterized by rapid sea-level fluctuations and non-optimal carbonate productivity had a significant area, intermediate between highstand and lowstand positions, that developed sequences with special characteristics that they termed build-and-fill sequences. A build-and-fill sequence is characterized by the following: either entirely a carbonate, or mixed carbonate-siliciclastic sequence; laterally extensive in distribution, but thin compared to amplitude of sea level change, and typically of even thickness; tends to drape paleotopography as an entire unit; is capped by a surface of subaerial exposure; has a topographic-relief-building phase; has a topographic-relief-filling phase (Franseen and Goldstein, 2004). Paleotopography and sea level change seem to be primary controls on the development of build-and-fill sequences (McKirahan et. al., 2003), although non-optimal carbonate productivity is now also thought to be a primary control (Franseen and Goldstein, 2007). Previous work on the TCC by Franseen and Goldstein, (2004) hypothesized a build-and-fill motif.

A goal of my study is to test the build-and-fill hypothesis by evaluating how substrate elevation, relative sea level, paleotopographic, and paleogeographic conditions control sequence stratigraphic characteristics of the TCC at two field locations within the Cabo de Gata volcanic province of southeast Spain; La Molata and La Rellana/Ricardillo.

GEOLOGIC SETTING

The La Molata and La Rellana/Ricardillo field areas are located in the northeastern portion of the Cabo de Gata volcanic province in southeastern Spain (Figure

1). The Betic Mountains to the northwest of the Cabo de Gata region formed during Alpine orogenesis and the volcanic highs in the Cabo de Gata region resulted from Neogene volcanic activity associated with transtension between the African and Iberian plates (Rehault et al., 1985; Sanz de Galdeano and Vera, 1992). The Neogene volcanic basement of the Cabo de Gata region is separated from the Mesozoic-Paleozoic metamorphic basement of the Betic range by the Carboneras fault, a major sinistral strike-slip fault system, to the northwest (Platt and Vissers, 1989; Montenant and Ott d'Estevou, 1990; Fernandez-Soler, 2001; Martin et al., 2003). The Neogene calc-alkaline volcanics that floor the Cabo de Gata region have been dated at 17 Ma to 6 Ma (Lopez-Ruiz and Rodriguez-Badiola, 1980; Serrano, 1992). The middle to late Miocene of the Cabo de Gata region was characterized by an archipelago of emergent highs and small submarine basins with interconnected straits and passageways formed through erosion and faulting of the volcanics (Esteban, 1979; Esteban and Giner, 1980; Sanz de Galdeano and Vera, 1992; Esteban, 1996; Franseen and Goldstein, 1996; Franseen et al., 1998). Heterozoan carbonate associations followed by photozoan carbonate associations, and finally TCC (Figure 2) were deposited on the flanks of the Neogene volcanic highs in the middle and late Miocene and have been the focus of numerous studies (Dabrio et al., 1981; Goldstein and Franseen, 1995; Whitesell, 1995; Esteban, 1996; Esteban et al., 1996; Franseen and Goldstein, 1996; Martin et al., 1996; Franseen et al., 1997a; Franseen et al., 1997b; Brachert et al., 1998; Franseen et al., 1998; Brachert et al., 2001; Martin et al., 2003; Toomey, 2003; Dillett, 2004; Martin et al., 2004; Johnson et al., 2005; Dvoretsky, 2009).

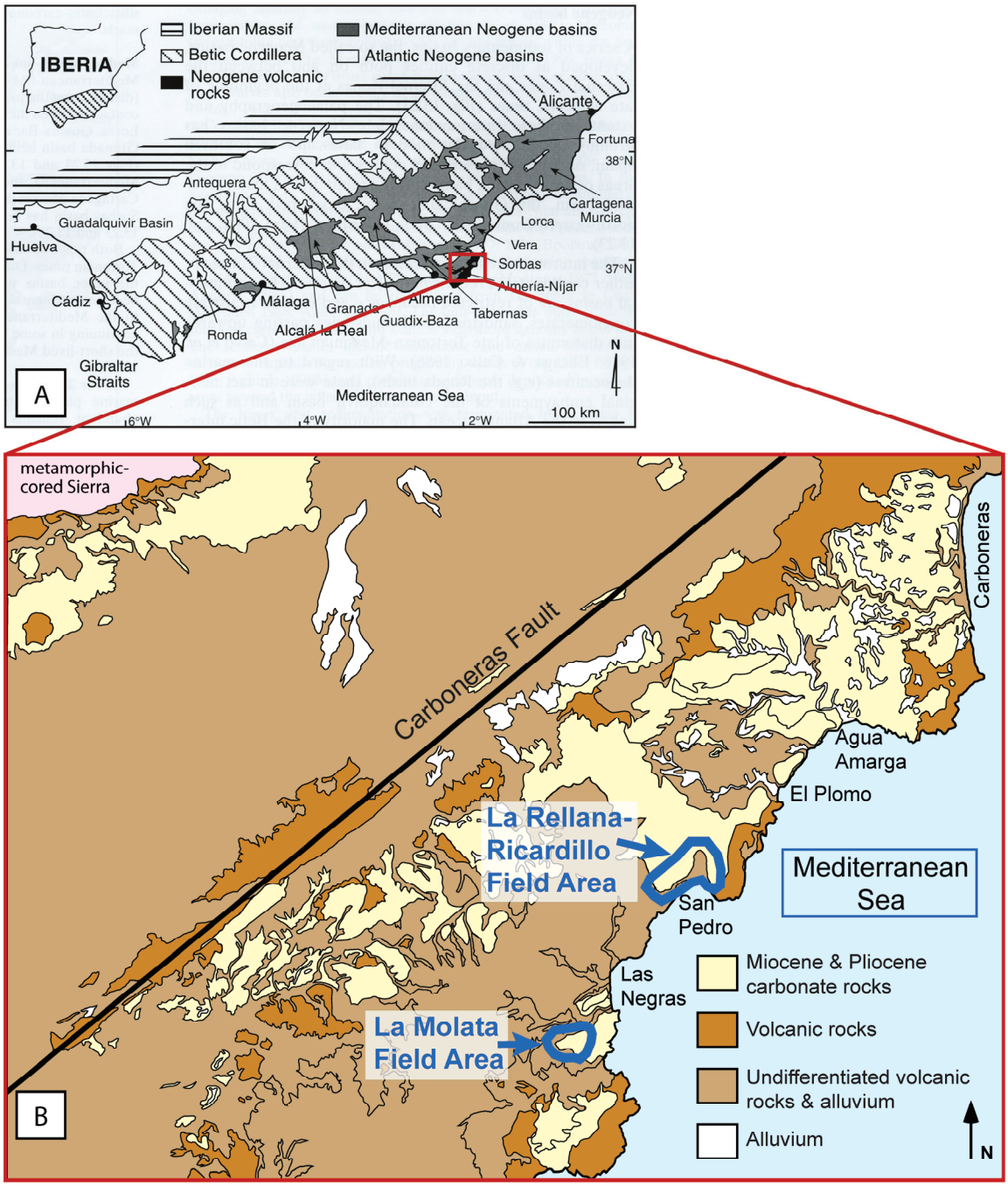

Figure 1: A. Location map of Neogene basins within the Betic Cordillera of southern Spain. Red Box outlines the Cabo de Gata volcanic province. *Modified from: Gibbons and Moreno, 2003.* B. Generalized geologic map of the Cabo de Gata region and location of the La Molata and La Rellana/Ricardillo field areas with the Carboneras fault to the west. *Modified from: Dvoretsky (2009).*

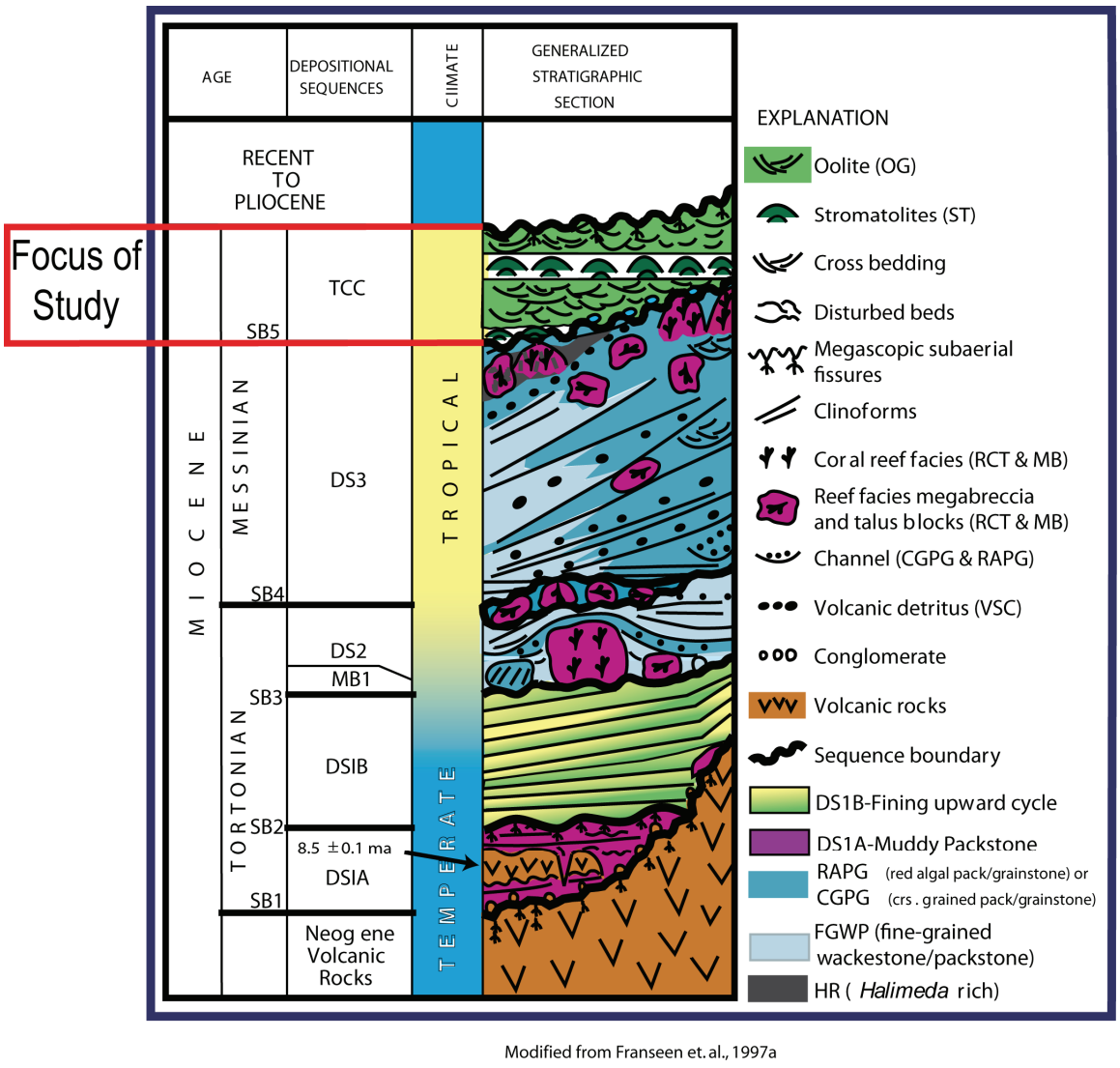

Modified from Franseen et. al., 1997a

Figure 2: General stratigraphy for Miocene carbonates in the Las Negras area.

An interbedded volcanic unit within the lower sequence (DS1A) of the Las Negras area gives an Ar/Ar date of 8.5 ± 0.1 Ma, thereby indicating a Tortonian age for earliest carbonate deposition in the area (Franseen et al., 1997a; Franseen et al., 1998). That radiometric date, integrated with biostratigraphy and magnetostratigraphy, provides a detailed chronostratigraphy for the entire section in the Las Negras area and indicates that sequences developed during Tortonian and Messinian time. On the basis of chronostratigraphy developed by Franseen et al. (1998) for the Las Negras area, and work of others, the TCC is approximately 5.8-5.3 MA in age and closely associated with the "Messinian Salinity Crisis".

During the Messinian of the Mediterranean Sea, Hsu et al. (1973, 1977) proposed a salinity crisis in the Mediterranean basin that led to thick evaporite deposition (Lower and Upper Evaporite Units) in the basins around the Mediterranean (Dronkert, 1976; Montadert, 1978; Esteban, 1979; Esteban and Giner, 1980; Dabrio et al., 1981; Riding et al., 1991; Rouchy and Saint Martin, 1992; Braga et al., 1995). The TCC was deposited on highs around the Mediterranean in shallow seas after, and possibly during, late stages of evaporite deposition in the adjacent basins. The TCC has been interpreted as the landward equivalent of the Upper Evaporite deposits during the Messinian based on stratigraphic relations, lack of diverse biota, and possible evaporitic molds within stromatolites (Montadert, 1978; Esteban, 1979; Esteban and Giner, 1980, Dabrio et al., 1981; Rouchy and Saint Martin, 1992; Martin and Braga, 1994). A cyclic nature has been identified within the Upper Evaporitic deposits throughout the Mediterranean (Dronkert, 1976; Valles Roca, 1986; Rouchy and Saint Martin, 1992).

Detailed studies of the Miocene carbonate outcrops from the Las Negras area (Esteban and Giner, 1980; Franseen and Mankiewicz, 1991; Franseen et al., 1993; Franseen and Goldstein, 1996; Franseen et al., 1997a; Franseen et al., 1998; Toomey, 2003; Johnson et al., 2005) , the Nijar basin (Dabrio et al., 1981; Mankiewicz, 1996), the Agua Amarga basin (Franseen et al., 1997b; Dvoretsky, 2009), and the Carboneras basin (Dillett, 2004) indicate that little deformation has affected the majority of carbonate strata in these areas and that paleotopography is largely preserved. Several studies, however, have documented pre-Messinian tectonic deformation in basins of southeastern Spain (Braga and Martin, 1988; Calvo et al., 1994; Cornee et al., 1994; Martin and Braga, 1994; Martin et al., 1996). It is generally accepted that during the Pliocene, uplift of the Betic Cordillera occurred with the interior parts of southeastern Spain uplifted more than the coastal regions (Sanz de Galdeano and Vera, 1992). In the Las Negras area, previous studies have shown that time-equivalent sequence boundaries are found at consistent elevations, there are no angular unconformities in the Messinian, numerous types of geopetal fabrics throughout the entire section are consistent with modern up direction, and most faults that cut across the Messinian carbonates have a maximum displacement of only a few meters (Esteban and Giner, 1980; Franseen and Mankiewicz, 1991; Franseen et al., 1993).

A regionally significant subaerial exposure surface (SB5 for the Las Negras area (Goldstein and Franseen, 1995)) overlies and erosionally truncates (estimated at 10's of meters) the DS3 unit (Reef Complex) of Franseen and Mankiewicz (1991), that formed the surface paleotopography for deposition of the TCC (Franseen et al., 1996). Evidence for subaerial exposure is well documented in previous studies and includes chalkification,

autoclastic brecciation, micritization, rhizoliths, laminated crusts, possible soil development, caliche, vertical fissures, circumgranular cracks, meniscus cements, and fenestrae (Esteban and Giner, 1980; Dabrio et al. 1981; Franseen and Mankiewicz, 1991; Whitesell, 1995; Franseen et al., 1996). In general, the resulting surface dips gently seaward and exhibits an irregular, hummocky morphology that likely reflects the local resistant lithologies below (Dabrio et al., 1981). In some instances, the surface morphology reflects marine terracing with wave cut notches (Dabrio et al., 1981).

Two field areas, 5 km apart, were studied in the Las Negras area. The La Molata field area includes the TCC outcrop on the top of an isolated hill, 0.86 by 0.43 km, on the eastern side of the Rodalquilar caldera (Arribas Jr. et al., 1995) with volcanic highs to the south, west, and north, and the Mediterranean Sea to the east (Figure 3). The Miocene carbonates unconformably overlie the volcanic basement rocks of La Molata. The TCC on La Molata ranges in thickness from 4–28.2 m and drapes and onlaps 33 m of relief, as traced laterally over the unconformity at its base. Previous studies of upper Miocene carbonates at La Molata identified cyclic sequences composed of stromatolite, thrombolite, oolite lithofacies (Franseen et al., 1993; Whitesell, 1995). Franseen et al. (1993) and Whitesell (1995) identified evidence for subaerial exposure at the top of sequences in the form of fenestral fabric, alveolar textures, rhizoliths, caliche-coated grains, micritized grains, fissures, truncated grains, laminated crusts, meniscus and pendant micrite cements.

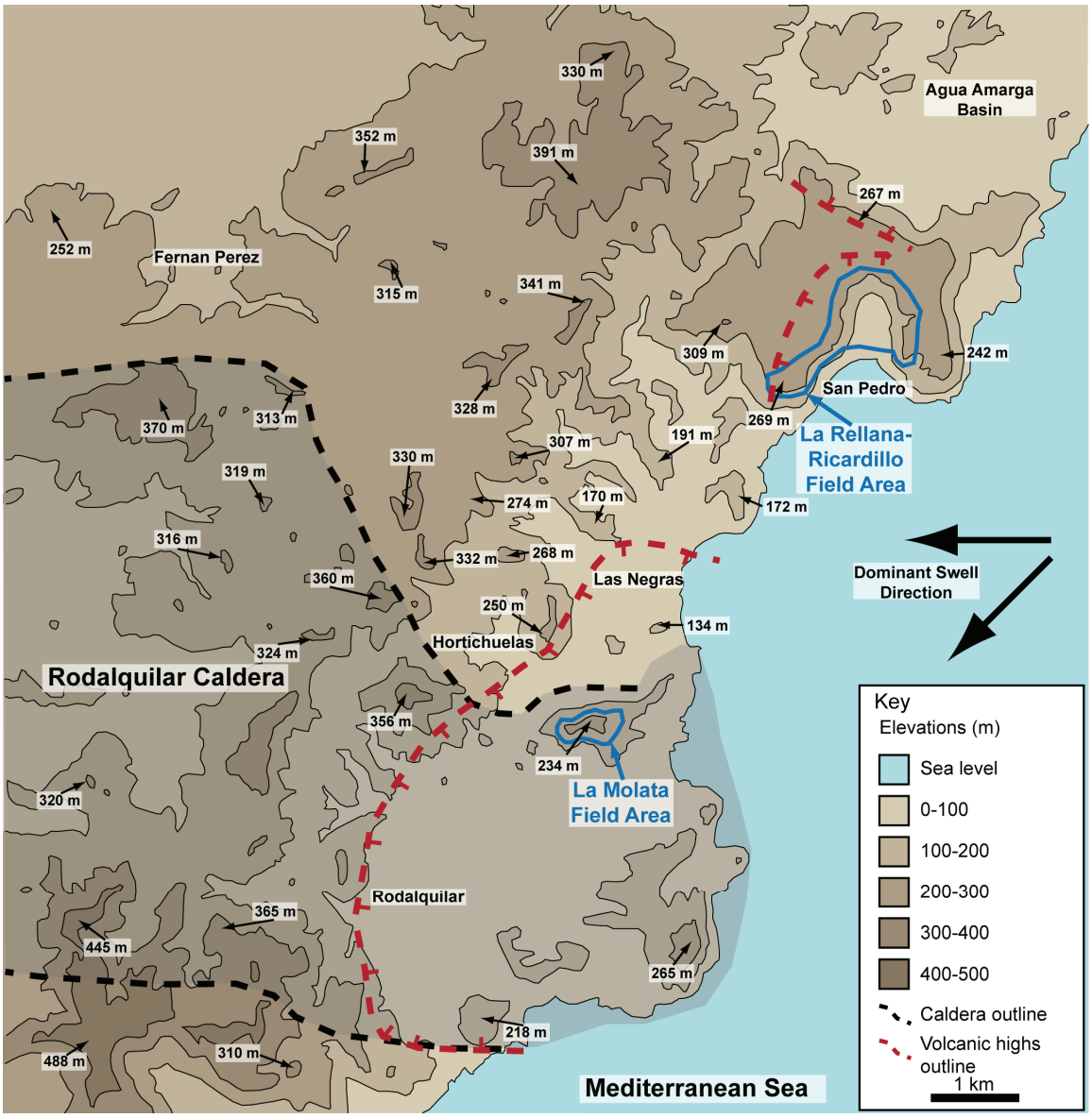

Figure 3: Topographic and paleogeographic map for the studied field areas. The La Molata field area is 0.86 X 0.43 km and encompasses the majority of TCC deposition in the area. Lowest elevation of the TCC is at 175 meters above present-day sea level. The basal unconformity climbs from that elevation to 208 m elevation. The highest exposure of the TCC crops out at 234 m elevation. La Molata is located on the northeastern margin of the Rodalquilar Caldera and surrounded by volcanic highs to the north, west, southwest, south, and southeast, with the Mediterranean Sea to the east. The caldera and volcanic highs surrounding La Molata created an embayment that protected the area, assuming east-southeast-directed swells. This caused marine conditions within the embayment to be more restricted. The La Rellana/Ricardillo field area encompasses an elongate area, 1.63 km long and 0.93 km at its widest point. The basal TCC surface crops out between 181 m and 257 m elevation with the highest TCC outcrop at 269 m elevation. Volcanic highs are to the northwest and west. The Agua Amarga basin is to the north with the Mediterranean Sea to the south and east. The La Rellana/Ricardillo field area is open to the east and north. This provided good connection with the main Mediterranean basin and direct exposure to a possible swell from the east-northeast. It also meant that the area would encounter the highest wave energy from the east-southeast currents. *Modified from Mapa Excursionis Y Turistico: Cabo de Gata Nijar Parque Natural; Rodalquilar Caldera location after Arribas et al., (1995); Dominant swell direction from modern Mediterranean (Lionello and Sanna, 2005).*

Cerro de Ricardillo is a dacitic volcanic dome that rises to more than 300 m in elevation (Fernandez-Soler, 1996). Miocene carbonates were deposited on its flanks and unconformably overlie the volcanic basement. The La Rellana/Ricardillo field area encompasses an elongate area, 1.63 km long and 0.93 km at its widest point. The TCC at La Rellana/Ricardillo ranges in thickness from 3.5–21.1 m and drapes and onlaps 76 m of paleotopographic relief as traced laterally along its basal unconformity. Volcanic highs are to the northwest and west of La Rellana/Ricardillo and the Mediterranean to the south and east (Figure 3). Toomey (2003) identified stromatolites, oolites, and *Porites* patch reefs in the TCC at La Rellana/Ricardillo.

METHODOLOGY

Field work was conducted on La Molata and La Rellana/Ricardillo from May to July in the summer of 2007 and consisted of measuring stratigraphic sections, mapping surfaces, lithofacies, and geometries on photomosaics, and collecting hand samples for core plug petrophysical and petrographic analysis.

Fifteen stratigraphic sections at La Molata and twenty-nine at La Rellana/Ricardillo provide a detailed 3D lithofacies framework for the TCC (Appendix I). The distribution of stratigraphic sections was based on the quality of exposure, accessibility of the outcrop, and spacing between sections. Contacts, lithofacies, and geometries were physically traced out in the field when possible or correlated with photomosaics (Appendix II). Approximately 450 hand samples were collected to represent the designated lithofacies, and for core plug and petrographic analysis. From the 450 hand samples, 399 core plugs were taken with 1 inch diameter and lengths

varying from 0.5-2 inches. The plugs were calibrated at the Kansas Geological Survey and sent to CoreLabs for Helium porosity, air and liquid permeability, and grain density measurements (Appendix III). Eighty-seven thin sections were made from the hand samples and core plugs for petrographic analysis. The majority of the thin sections were made by Spectrum Petrographics, Inc. with the minority being made at the University of Kansas by Wayne Dickerson. The thin sections were studied at the University of Kansas using a petrographic microscope. (Appendix IV).

PALEOTOPOGRAPHY

Data for paleotopographic reconstruction of the basement surface of TCC deposition (TCC/DS3 contact) included physically tracing and mapping the surface on photomosaics, marking the contact on a topographic map using a Brunton compass, and collecting UTM coordinates using a hand-held GPS unit. These data were brought into Petrel™ within wells created from the 44 measured stratigraphic sections and 125 pseudo wells created from the photomosaics, topographic maps, and recorded UTM coordinates. Stratigraphic picks were made and correlated for the wells on the TCC/DS3, contact and a surface was created from the picks using a convergent interpolation algorithm.

On La Molata, three possible normal faults cut through the TCC and represent the extent of deformation in the area (Appendix V). The largest of the three is found east of the central high and can be identified from both the southern and northern sides of the hill. The strata are offset by approximately 5 meters and dips of beds increase, locally about 20 degrees immediately near the fault. On the south side of the hill there is a possible fault that offsets the strata approximately 1.5 meters. The north side has a

possible fault with approximately 1 meter of offset. La Rellana/Ricardillo has three possible normal faults with two on the south end of La Rellana and one on the southwestern end of Cerro de Ricardillo. These faults represent the extent of deformation involving TCC strata in the area (Appendix VI). The larger of the two faults at La Rellana offsets the strata by just less than 7 meters. The smaller of the two faults offsets the strata by less than 4 meters and may affect the dips of the beds near the fault. On Cerro de Ricardillo, the possible normal fault offsets the strata by approximately 4 meters. All the faults in the field areas are post-TCC deposition and were ignored when reconstructing the paleotopography for the field areas.

The paleotopographic maps illustrated in Figure 4 represent the resulting surface elevations (in meters above present-day sea level) on top of DS3 at La Molata and La Rellana/Ricardillo. Small patches of TCC that may be preserved basinward of La Molata between 60–90 m substrate elevations were not included for this study. At La Molata, the paleotopographic high point is located on the northern side of the central high at 208 m elevation. The surface dips gently to the west, south, and east from the central high and averages between 2–5 degrees with local irregularities due to more or less resistant lithologies below (Appendix VII). The west side drops to an elevation of 201 m and the east side drops to 175 m. Two major paleovalleys are observed, one on the east side and the other on the northeast side, that affected subsequent deposition of TCC lithologies (Figure 4A).

The paleotopographic high point for the La Rellana/Ricardillo field area is at 257 m elevation in the northwest portion of the Cerro de Ricardillo and the low point is at 181

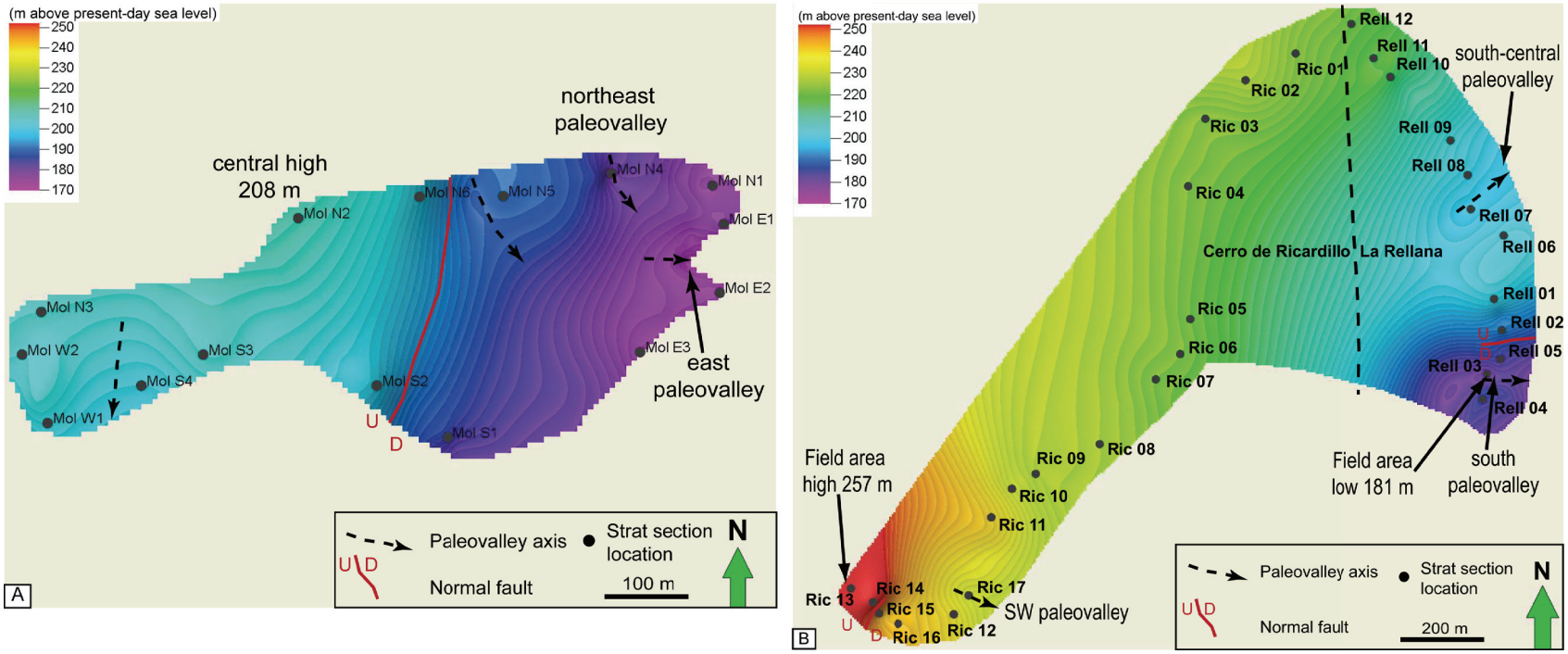

Figure 4: A. Paleotopographic map of the surface onto which the TCC was deposited at La Molata. The paleotopographic high point is located at the center of the hill on its northern side and is 208 m above present-day sea level. The surface gently dips from the central high to the east, south, and west with local variations. The west margin drops to 201 m elevation and the east to 175 m elevation. Two major paleovalleys are observed that affected deposition, one on the east side and one near the northeast margin. B. Paleotopographic map of the surface onto which the TCC was deposited at La Rellana/Ricardillo. The high is located at the northwest margin of Cerro de Ricardillo at 257 m elevation. The low is located on the southern margin of La Rellana at 181 m elevation. In general, the surface dips gently (1-9 degrees commonly) from the high to the east and southeast on Cerro de Ricardillo. A paleovalley was located at the southwest portion of Cerro de Ricardillo. In the La Rellana area, the surface dips gently (1-6 degrees commonly) to the south and southeast. Two paleovalleys were present during TCC deposition with one centrally located and the other near the southern margin.

m elevation near the southern margin of La Rellana. In general, the surface dips gently (1-9 degrees commonly) from the high to the east and southeast on Cerro de Ricardillo (Appendix VIII). In the La Rellana area, the surface dips gently (1-6 degrees commonly) to the south and southeast with dips becoming steeper (up to 11 degrees) south of the pronounced break in slope at the southern margin (Appendix VIII). Three paleovalleys observed in the La Rellana/Ricardillo field area affected subsequent TCC deposition (Figure 4B). One paleovalley is in the southwest portion of Cerro de Ricardillo and two at La Rellana, one in the central portion and one near the southern margin.

Interpretation

The surface paleotopography that the TCC was deposited on was sculpted by subaerial erosion. Reef buttresses within the DS3 unit are locally immediately below the TCC basal surface. The erosion surface is locally higher in sections Mol N5 and Rell 04, where reef buttresses are located. The less resistant DS3 lithologies are on all sides of the buttresses. As the reefs form paleohighs on the surface, those paleohighs likely result from the reefal facies' greater resistance to subaerial erosion than other facies. The paleovalleys on the surface likely preserve the paleodrainage system formed during subaerial exposure.

LITHOFACIES

As indicated previously, the TCC consists of four cyclic sequences that are designated herein as Sequence 1, Sequence 2, Sequence 3, and Sequence 4. Each sequence consists of lithofacies that, in general, are repetitive in a vertical sense from the base to the top of each sequence, but show differences especially in relation to elevation.

Figures 5 and 6 show the generalized stratigraphy for the TCC at the La Molata and La Rellana/Ricardillo field areas in relation to elevation. For low elevations, a typical sequence has local basal stromatolites overlain by local thrombolite boundstone, that upward, becomes interbedded with and eventually overlain by trough cross-bedded ooid grainstone. Trough cross-bedded ooid grainstone grades upward to volcaniclastic-rich planar bedded ooid grainstone that is capped by fenestral ooid grainstone. For high elevations, a typical sequence has local basal stromatolites overlain by local thrombolite boundstone that is overlain by trough cross-bedded ooid grainstone. Where stromatolites and thrombolite boundstone are absent, trough cross-bedded ooid grainstone is the basal lithofacies. Trough cross-bedded ooid grainstone grades upward to volcaniclastic-rich planar bedded ooid grainstone that is capped by fenestral ooid grainstone.

Trough Cross-bedded Ooid Grainstone

The trough cross-bedded ooid grainstone (Table 1; Appendix IX) is volumetrically the most abundant lithofacies at both field areas, and accumulations range in thickness from 0.66-11.1 m (thickest in Sequence 3). The lithofacies is present in all the sequences at both locations. Master bedding is on the meter-scale and drapes or onlaps, paleotopography. The trough cross-beds (Figure 7A) are meter-scale (commonly < 2 m wide) and the cross-stratification is very thinly bedded. Ooids are the predominant grain type, ranging between 80-99 percent. The amount of skeletal grains and volcaniclastic grains vary between sequences and field locations. Dominant skeletal grains are gastropods and bivalves, with lesser amounts of benthic forams and serpulid worms. Skeletal grains are highly abraded, and commonly preserved as fragments with

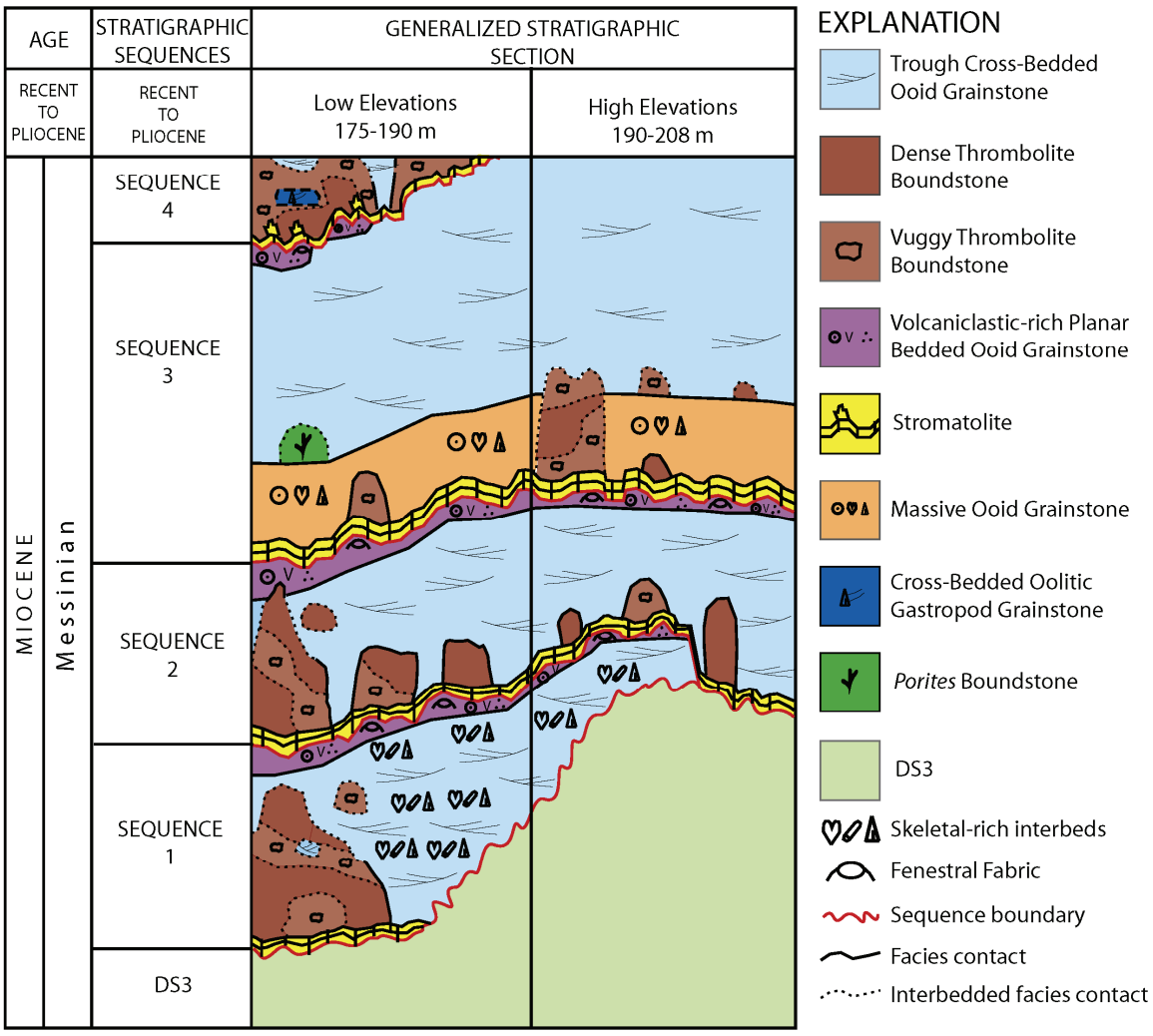

Figure 5: La Molata TCC general stratigraphy and lithofacies distributions in relation to elevation.

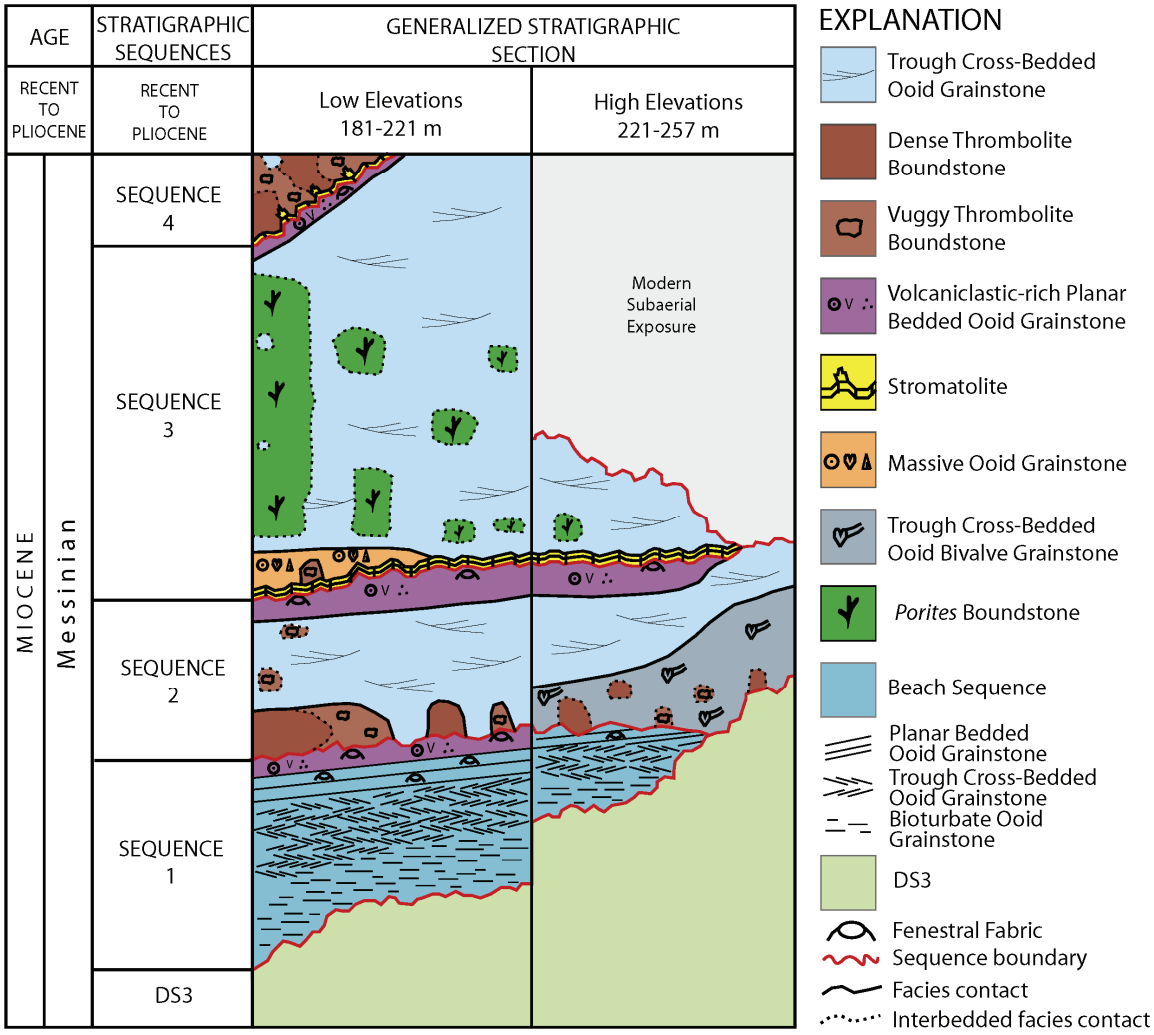

Figure 6: La Rellana/Ricardillo general stratigraphy and lithofacies distribution in relation to elevation.

Lithofacies Classification	Key features	Characteristic grain types	Prominent structures, bedding, and thickness	Depositional environment
Trough cross-bedded ooid grainstone	Trough cross-beds	80-99% ooids (0.4-0.8 mm), gastropods (20-90% in interbeds), bivalves (5-15% in interbeds), serpulid worms (35-95% in interbeds)	Troughs generally oriented N-S or S-N; S1 interbeds 1-3 cm thick; unit thickness 0.66-11.1 m	High energy, < 10 m water depth, shoreface beach envir.
Bioturbate ooid grainstone	Dis-continuous laminations and burrows	80-99% ooids (0.15-0.75 mm), gastropods (20-60% interbeds), bivalves (10-20 % interbeds), serpulid worms (10-95% interbeds)	Common discontinuous laminae; interbeds commonly 1-4 cm; common burrows; unit thickness 0.2-1.4 m	Low-moderate energy, offshore envir. > 10 m
Planar bedded ooid grainstone	Planar beds; <5% volcani-clastic grains	81-99% ooids (.2-1.2 mm), gastropods (1-10% interbeds), bivalves (5-15% interbeds), serpulid worms (45-95% interbeds), 0-5% volc. grains	Decimeter-scale planar beds shallowly dip 1-11 degrees; alternating coarser/finer very thin beds; unit thickness 0.28-0.93 m; fenestrae	Moderate-high energy, < 2 m water depth, foreshore beach envir.
Massive ooid grainstone	Lack of bedding	79-99% ooids (0.15-2 mm, pisoids up to 3mm), bivalves, gastropods, serpulid worms	Common burrows; larger grain sizes; poorer sorting; unit thickness 0.83-2.11 m	Low-moderate energy, > 10 m depth
Volcaniclastic-rich planar bedded ooid grainstone	Planar beds; >5% volcani-clastic grains	75-95% ooids (0.16-1.2 mm), 5-16% volc. grains (0.4-12 mm)	Decimeter-scale planar beds shallowly dip 2-7 degrees, fenestrae high in section, unit thickness 0.24-3.1 m	Moderate-high energy, < 3 m depth, foreshore beach envir.
Fenestral ooid grainstone	Dominant fenestral fabric	75-99% ooids (0.2-1.1 mm), volc. grains	Fenestrae; rhizoliths; meniscus cements; unit thickness 0.1-0.4 m	Subaerial exposure
Cross-bedded oolitic gastropod grainstone	Abundant gastropods; cross-stratification	Ooids, 17-72% (commonly 30-60%) gastropods, peloids	Tabular cross-beds; possible microbial influence, unit thickness 0.47-1.3 m	Moderate-high energy, shallow, near-shore envir.
Trough cross-bedded ooid bivalve grainstone	Abundant bivalves; trough cross-beds	50-75% ooids (0.15-0.65 mm), 15-30% (up to 90 locally at base) bivalves, 4-12% volc. grains	Trough cross-beds; interbedded with thrombolite boundstone; unit thickness 0.71-5.2 m	High energy, < 10m water depth, near-shore envir.
Thrombolite boundstone	Dark clotted texture	Commonly 15-60% peloids, gastropods, bivalves, ooids, calc. red algae, serpulid worms	Clotted texture made of peloids; unit thickness 0.27-5 m	High energy, shallow, near-shore envir.
Stromatolite	Fine planar laminae; rare digitate (S4); micrite	Up to 60% peloids, ooids, 5-15% volc. grains	Finely laminated; clotted texture; alternating coarser/finer laminae; unit thickness 0.05-0.7 m	Low-high energy; shallow near-shore envir.
Porites boundstone	Abundant *Porites;* micrite	*Porites*, gastropods, bivalves, serpulid worms, ooids, calc. red algae, clionid sponges, peloids	Massive coral heads 1-3 m wide and 2-3 m thick; unit thickness 0.64-6.2 m	High energy, <10 m water depth

Table 1: Summary chart of diagnostic features for lithofacies within the study areas. Detailed lithofacies constituents are found in Appendix IX. Grain types are listed in order of abundance. Sx=Sequence X, volc.=volcaniclastic, calc.=calcareous, envir.=environment

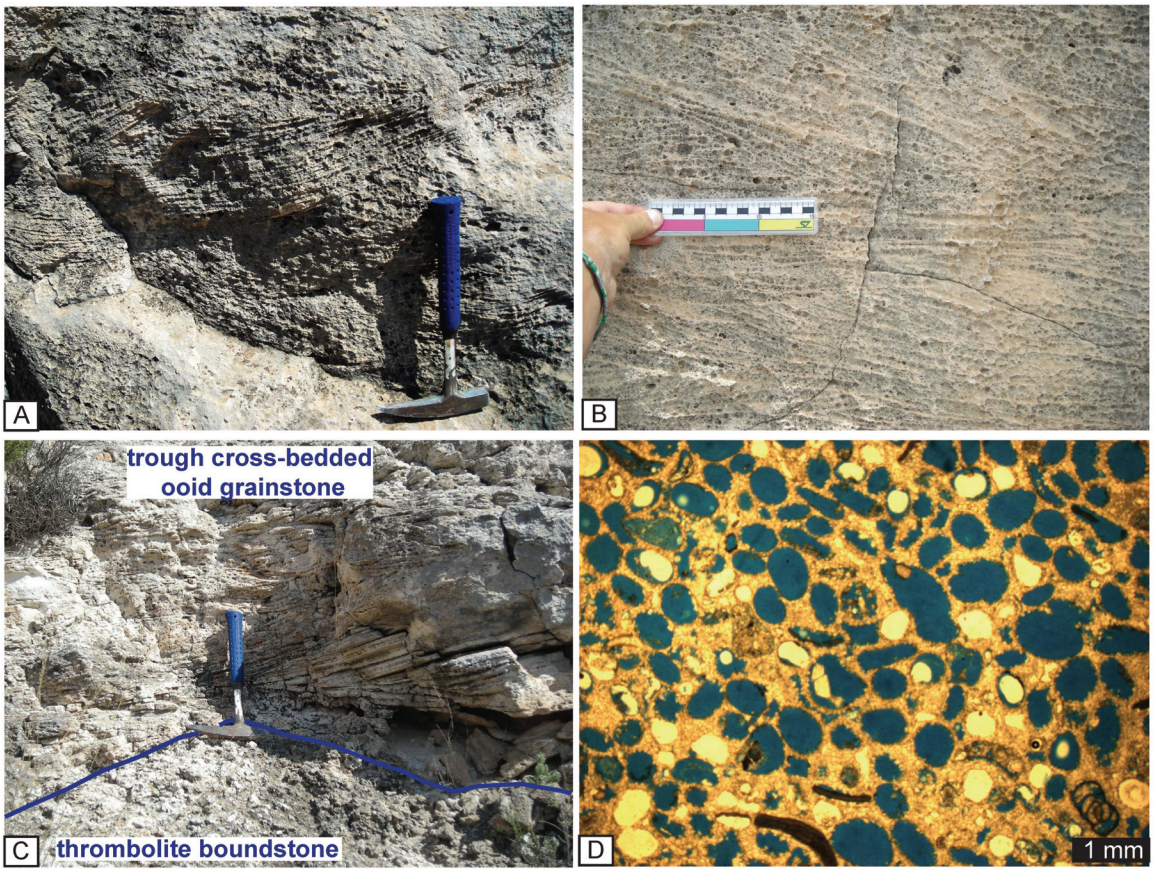

Figure 7: Trough cross-bedded ooid grainstone photographs and photomicrograph. Hammer is 32 cm long and field scale is marked in centimeter increments with black and white bars. Scale for photomicrograph is in the right corner and is 1 mm. A. Troughs are the characteristic feature of the lithofacies and are commonly on the meter-scale. B. Tabular cross-stratification is more common higher in section of the sequences. C. Trough cross-bedded ooid grainstone laps out against thrombolite boundstone that is stratigraphically lower. The contact is sharp and locally erosive. D. Photomicrograph showing the common oomolds within the lithofacies. Ooids are commonly 0.4-0.8 mm in size. Benthic forams (*Quinqueloculina* and *Spiroloculina)* are rare to common within the lithofacies.

rare whole grains. Volcaniclastic grains range from rare to common and peloids are rare. The grains are well sorted. In Sequence 1 of both field areas, very thin interbeds average 1-3 cm in thickness and contain greater concentrations of gastropods, bivalves, and serpulid worm fragments. In Sequences 2 and 3 of La Rellana/Ricardillo, skeletal grains are more common than at La Molata. Sequence 3 at La Rellana/Ricardillo commonly has burrows.

Interpretation

Modern ooids are generally deposited in high-energy environments in water depths less than 10 m, with the most significant ooid generation occurring in 2 m or less water depth (Ball, 1967; Loreau and Purser, 1973; Hine, 1977; Flugel, 1982; Harris, 1983; Lloyd et al., 1987; Tucker and Wright, 1990; Burchette and Wright, 1992; Major et al., 1996). Trough cross beds are a common sedimentary structure above fair-weather wave base (Burchette and Wright, 1992; Boggs, 1995; Wright and Burchette, 1996). In the modern Mediterranean, fair-weather wave base commonly does not reach below 8 m water depth (Fornos and Ahr, 1997). The modern is the best analog for the Mediterranean during the Miocene and fair-weather wave base was likely at a similar water depth. The lack of mud, abundant ooids, highly abraded grains, and good sorting indicate that the lithofacies was deposited in high energy conditions. Trough cross-beds are common in the shoreface of beach environments and oolitic coatings are commonly thickest in the shoreface (Inden and Moore, 1983). At La Rellana/Ricardillo, Sequence 1 has common tabular cross-beds and trough cross-beds that scour into lower beds. Within the cross-

stratification, alternating coarser and finer very thin beds are similar to features described by Inden and Moore (1983) that indicate deposition in a beach environment.

Given these characteristics, as well as the fact that the volcaniclastic-rich planar bedded ooid grainstone lithofacies is the updip equivalent, this lithofacies is interpreted to have been deposited in the shoreface of a beach environment within fair-weather wave-base (likely less than 10 m) (Inden and Moore, 1983).

Bioturbate Ooid Grainstone

The bioturbate ooid grainstone lithofacies (Table 1; Appendix IX) is the basal lithofacies in Sequence 1 at La Rellana/Ricardillo and ranges from 0.2-1.4 m in thickness. Laminae are common but discontinuous (Figure 8B) due to bioturbation. Ooids are the dominant grain type ranging between 80–99 percent. Skeletal grains include abundant gastropod, bivalve, and serpulid worm fragments with rare benthic forams. Skeletal grains are preserved whole and as fragments with moderate abrasion. Volcaniclastic grains and peloids are rare. The bioturbate lithofacies has 1-3 cm thick very thin interbeds with greater concentrations of skeletal grains, similar to the trough cross-bedded lithofacies of Sequence 1. The grains within the lithofacies are moderate to well sorted.

Interpretation

The bioturbate ooid grainstone is a downdip equivalent of the trough cross-bedded ooid grainstone, thereby indicating a deeper depositional environment. The planar laminations suggest that the ooids were transported. The abundance of ooids suggests that the ooids were originally formed in a nearby environment. Bioturbation suggests relatively low

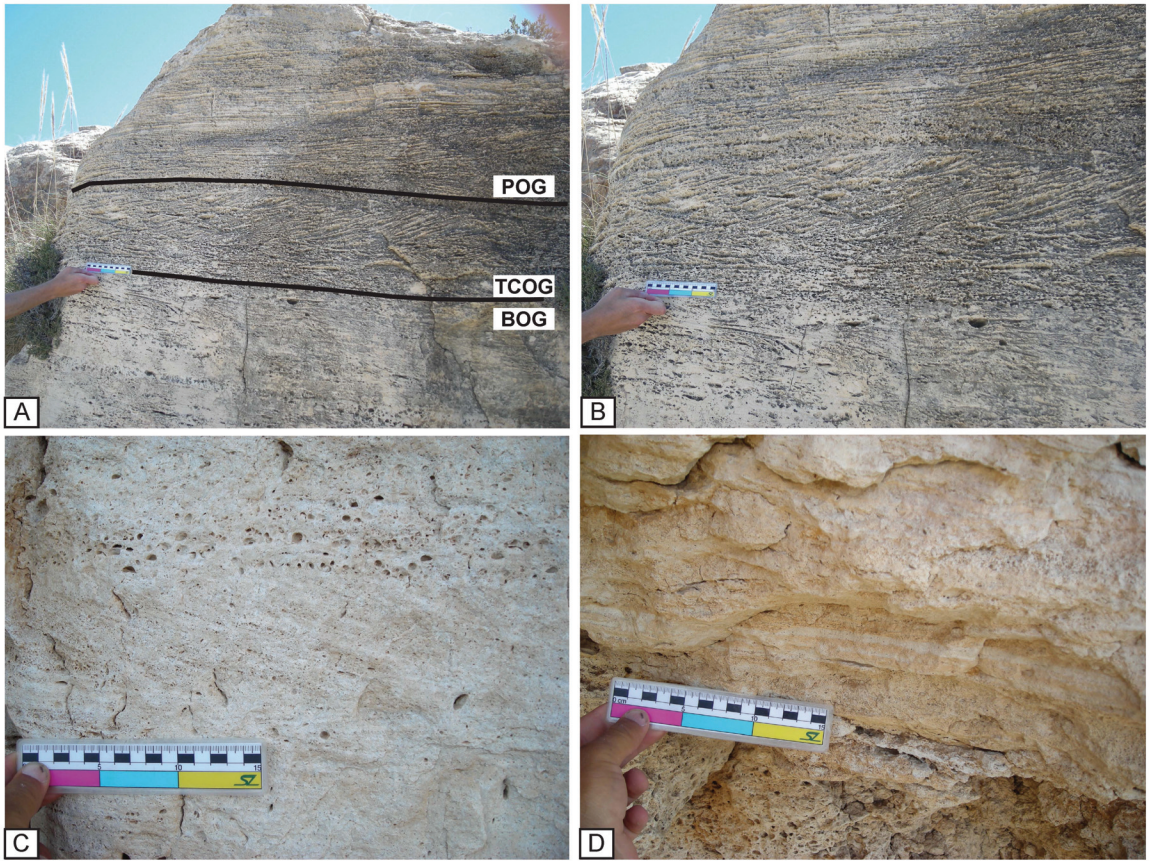

Figure 8: Lithofacies photographs for the beach sequence in Sequence 1 at La Rellana/Ricardillo field area. Field scale is marked in centimeter increments with black and white bars. A. Textbook beach sequence with bioturbate ooid grainstone (BOG) transitioning upward to trough cross-bedded ooid grainstone (TCOB) and then to planar bedded ooid grainstone (POG). BOG has discontinuous laminae and common burrows. Very thin skeletal-rich interbeds (commonly 1-3 cm) are in all the lithofacies. B. Closer view of the beach sequence showing the discontinuous laminae of the BOG, trough cross-stratification of the TCOG and shallowly dipping planar beds of the POG. C. All the lithofacies of the beach sequence contain interbeds of gastropods, bivalves, and serpulid worm fragments. This photo is from the TCOG and shows the alternating coarse/fine grained laminations. D. Alternating coarse/fine grained laminations in the BOG highlighted by darker and lighter color.

energy conditions below fair-weather wave base (Inden and Moore, 1983). Given the stratigraphic position, similar biota as in the trough cross-bedded ooid grainstone of Sequence 1, the abundance of ooids, lack of mud, and bioturbation, this lithofacies is interpreted to have been deposited in an offshore beach environment (>10 m water depth) with moderate to low energy conditions (Inden and Moore, 1983).

Planar Bedded Ooid Grainstone

The planar bedded ooid grainstone (Table 1; Appendix IX) occurs only in Sequence 1 at La Rellana/Ricardillo, and ranges from 0.28-0.93 m in thickness. Planar beds are on the decimeter-scale and dip shallowly (1-11°) to the southeast. Ooids are the dominant grain type ranging between 80–99 percent. Skeletal grains include abundant gastropod, bivalve, and serpulid worm fragments with rare benthic forams. Skeletal grains are rarely preserved whole and are highly abraded. The planar bedded ooid grainstone lithofacies has 1-3 cm thick very thin interbeds with greater concentrations of serpulid worm fragments. Grains are very well to well sorted. Alternating coarser and finer grained very thin beds consisting of ooids and skeletal grains are common (Figure 8C). Cross stratification is rare. Beach bubble fenestrae are rare to common, becoming more common stratigraphically higher in the sequence.

Interpretation

The planar bedded ooid grainstone is an updip equivalent of the trough cross-bedded ooid grainstone, indicating deposition in shallower water depths. The abundance of ooids, lack of mud, highly abraded grains, and presence of fenestrae indicate deposited in shallow water depths (likely < 2 m), with moderate to high energy conditions. The

position upslope from trough cross bedded oolite grainstone, shallowly dipping planar beds (dipping towards modern Mediterranean), rare cross-beds, and alternating coarse/fine grained very thin interbeds, support deposition within the swash zone of a foreshore beach environment (Ball, 1967; Inden and Moore, 1983).

Massive Ooid Grainstone

The massive ooid grainstone lithofacies (Table 1; Appendix IX) occurs only in Sequence 3 and ranges in thickness from 0.83-2.11 m. The lithofacies is characterized by lack of bedding. Faint planar laminations are rare and occur mostly at the La Rellana/Ricardillo field location. Burrows are common within the lithofacies. The massive ooid grainstone is moderately to well sorted. Ooids are the dominant grain type ranging between 80–99 percent. As compared to the other oolite lithofacies, the ooids are larger (commonly 0.6-2 mm) and some pisoids occur that are as large as 3 mm. Gastropod and bivalve grains are more abundant and larger in size (commonly 6-20% and 3-14 mm) as compared to the other oolites (Figure 9B). Serpulid worms, benthic forams, volcaniclastic grains, and peloids are all rare to common. Solitary corals, *Porites* boundstone, and *Tarbellastrea* are rare. The skeletal grains are preserved whole and as fragments with moderate abrasion.

Interpretation

The massive ooid grainstone is the downdip equivalent of the trough cross-bedded ooid grainstone lithofacies, thereby indicating a deeper depositional environment. The local preservation of faint planar laminations suggests that the ooids were transported, and the abundance of ooids suggests that the ooids were formed nearby. The prevalence

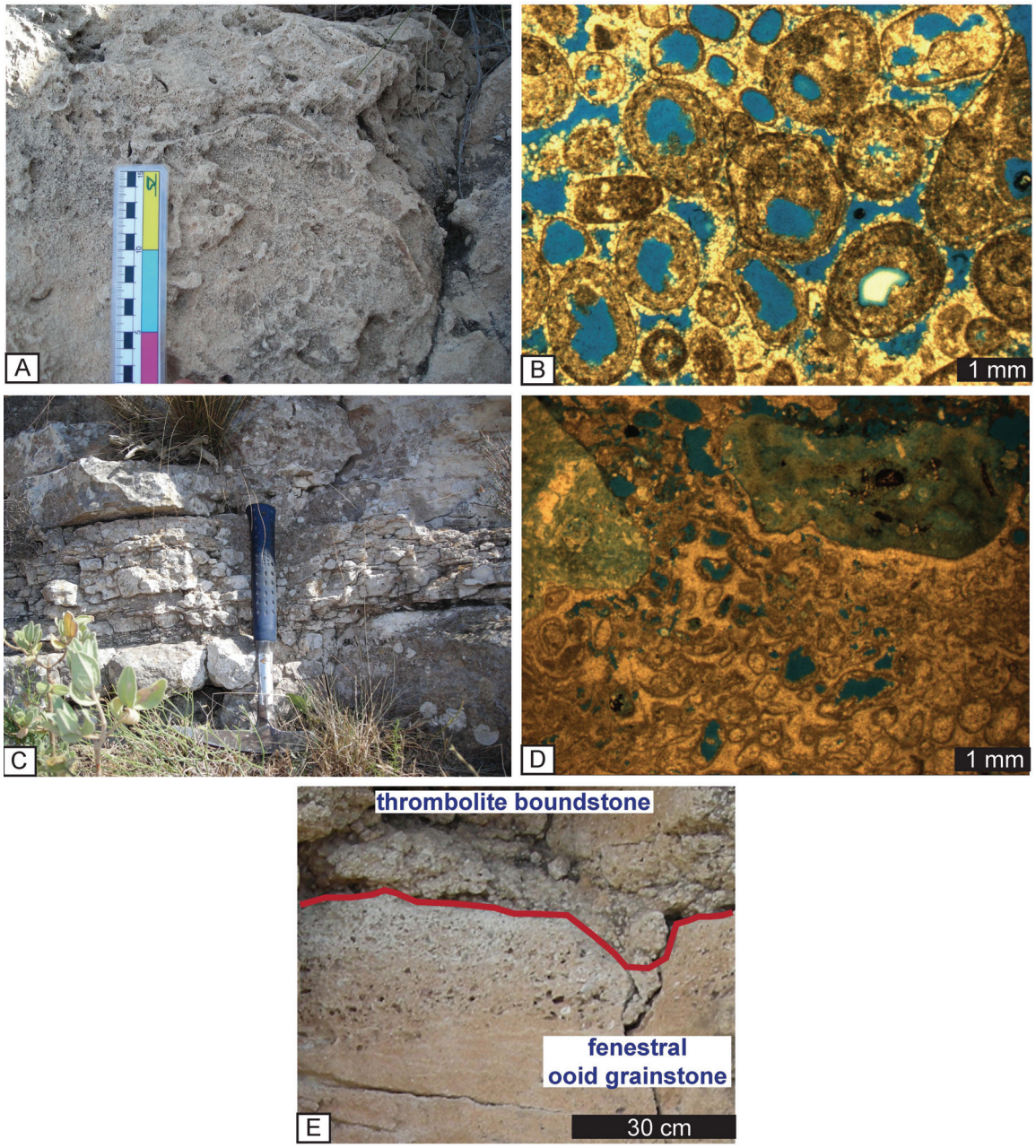

Figure 9: Lithofacies photographs and photomicrographs. Hammer is 32 cm long and field scale is marked in centimeter increments with black and white bars. Scales for photomicrographs are in the right corner and are 1 mm. A. Photograph of the massive ooid grainstone (MOG) lithofacies characterized by lack of bedding. Both vertical and horizontal burrows are common. B. Photomicrograph of the MOG lithofacies showing abundant large ooids (1.2-2.0 mm common) with some pisoids up to 3 mm. Composite grains and oomolds are common. C. Photograph of the volcaniclastic-rich planar bedded ooid grainstone (VPOG) showing the decimeter-scale, shallowly dipping planar beds. D. Photomicrograph of VPOG distinguished by abundance of volcaniclastic grains. E. Photograph of the fenestral ooid grainstone (FOG) lithofacies that locally caps sequences and is characterized by fenestral fabric. Red line marks sequence boundary.

of burrows suggests relatively low energy conditions below fair-weather wave base (Inden and Moore, 1983). This evidence in combination with the lack of mud and poorer sorting as compared to the trough cross-bedded ooid grainstone leads to the interpretation of deposition in a low to moderate energy environment in water depths greater than 10 m.

Volcaniclastic-rich Planar Bedded Ooid Grainstone

The volcaniclastic-rich planar bedded ooid grainstone lithofacies (Table 1; Appendix IX) ranges in thickness from 0.24-3.7 m and is present in Sequences 1, 2, and 3 at both locations. The lithofacies is characterized by gently dipping (~2-7° average, up to 15°) decimeter-scale planar bedding (rare cross-stratification), and greater than 5 percent volcaniclastic grains. Grains are moderately to very well sorted. Ooids are the dominant grain type ranging between 75 – 95 percent. Superficial ooids are more common than in the trough cross-bedded ooid grainstone lithofacies. This lithofacies contains more abundant and larger volcaniclastic grains (5-25% and 0.4-12 mm) than the other oolite lithofacies (Figure 9D). Volcaniclastic grains are also more common as cores of ooids than in the other oolite lithofacies. Peloids and skeletal grains, including gastropods, bivalves, serpulid worms and benthic forams, are rare. Volcaniclastic grains gradually become more abundant and larger in size stratigraphically higher in the sequences. Fenestrae are rare, but become more common stratigraphically higher in the sequences.

Interpretation

The volcaniclastic-rich planar bedded ooid grainstone is the updip equivalent of the trough cross-bedded ooid grainstone indicating shallower water depth for deposition (likely < 3 m). The greater abundance of volcaniclastic grains indicates deposition in the

shallowest waters in a near-shore environment. Lithofacies deposited in the shallowest water depths of a near-shore environment would have been nearer to the eroding, exposed volcanic highs. These lithofacies would be expected to have higher percentages of volcaniclastic grains. The shallowly dipping planar beds, planar bedding with rare cross-bedding, greater abundance of superficial ooids, and lack of mud indicate moderate to high energy of deposition within the foreshore of a beach environment (Ball, 1967; Inden and Moore, 1983). The presence of fenestrae suggests that these may be preserved beach accretion beds (Inden and Moore, 1983).

Fenestral Ooid Grainstone

The fenestral ooid grainstone (Table 1) ranges in thickness from 0.1-0.4 m and locally caps the sequences. The lithofacies is characterized by a dominant fenestral fabric (Figure 9E). Although mostly obscured by poor outcrop, bedding appears to be commonly planar bedded, and cross-bedding is rare. Ooids are the dominant grain type ranging between 75-99 percent. Volcaniclastic grains are rare to common. Peloids and skeletal grains, including gastropods, bivalves, serpulid worms and benthic forams, are rare. The lithofacies is commonly chalky, friable, and contains abundant fenestrae near the stratigraphic top of the sequences with less common rhizoliths, meniscus cements, possible caliche pisoids, and iron-stained grains.

Interpretation

Fenestrae, chalkification, rhizoliths, caliche pisoids, iron-stained grains, and meniscus cements can all be interpreted as evidence for subaerial exposure (Esteban and Klappa, 1983). The abundance of fenestrae, common planar bedding with rare cross-

stratification, and lack of mud indicate deposition in the immediate foreshore and possible backshore of a beach environment (Ball, 1967; Inden and Moore, 1983). The lithofacies is interpreted to be the result of deposition in a beach environment followed by alteration during subaerial exposure.

Cross-bedded Oolitic Gastropod Grainstone

The cross-bedded oolitic gastropod grainstone (Table 1; Appendix IX) ranges in thickness from 0.47-1.3 m and only occurs in Sequence 4 at La Molata. Tabular cross-beds are dominant with trough cross-beds less common. Cross-bedding is on the decimeter scale. The lithofacies is characterized by the abundance of gastropod grains (commonly 30-60%). The gastropods are preserved whole and are moderately abraded with < 5% having oolitic coatings. Ooids are abundant and peloids are common. In thin section, a clotted texture composed of peloids makes up portions of the lithofacies.

Interpretation

The cross-bedded oolitic gastropod grainstone is interbedded with thrombolite boundstone. The clotted peloidal texture is interpreted to result from microbial influence, which is also supported by the close relationship with thrombolite boundstone. The cross-stratification and abundant ooids, suggest deposition in shallow water depths (< 10 m) with moderate to high energy (Ball, 1967; Inden and Moore, 1983). However, the associated thrombolite boundstone, which formed bioherms, may have acted to focus current energy between bioherms and resulted in increased energy in water depths greater than 10 m. The greater abundance of gastropod grains without oolitic coatings and lesser amount of ooids as compared to the other oolite lithofacies may indicate that these grains

were transported from shallower water. Therefore, the cross-bedded oolitic gastropod grainstone is interpreted to have been deposited in water depths of 10 m or more.

Trough Cross-bedded Ooid Bivalve Grainstone

The trough cross-bedded ooid bivalve grainstone (Table 1; Appendix IX) ranges in thickness from 0.71-5.2 m, with the thickest accumulations occurring at the highest elevations of La Rellana/Ricardillo, and only occurs in Sequence 2. Master bedding thickness is on the meter-scale. The trough cross-beds are meter-scaled (commonly <2 m) (Figure 10A). Overall, ooids are the most abundant grain type averaging between 50 – 75 percent. Bivalves, which characterize this lithofacies (average between 15-30%), are more abundant and usually larger (0.5-20 mm) stratigraphically lower in the sequence, and can make up 90% of the grains within the lithofacies. The bivalves are commonly preserved as individual valves and are moderately abraded. Volcaniclastic grains are common, more abundant than in other cross-bedded oolite lithofacies, and are higher in concentration stratigraphically lower in the sequence (4-12%). The volcaniclastic grains are also more common as cores of ooids than in other cross-bedded oolite lithofacies. Gastropods and peloids are rare.

Interpretation

The trough-cross beds, lack of mud, abundance of ooids, and thick oolitic coats on the grains indicate high-energy and shallow water depths (< 10 m) for deposition (Ball, 1967; Inden and Moore, 1983). The abundance of volcaniclastic grains as cores for ooids and as grains indicates deposition in shallow water depths in a near-shore environment. The moderate abrasion of the bivalves suggests deposition outside of the highest energy

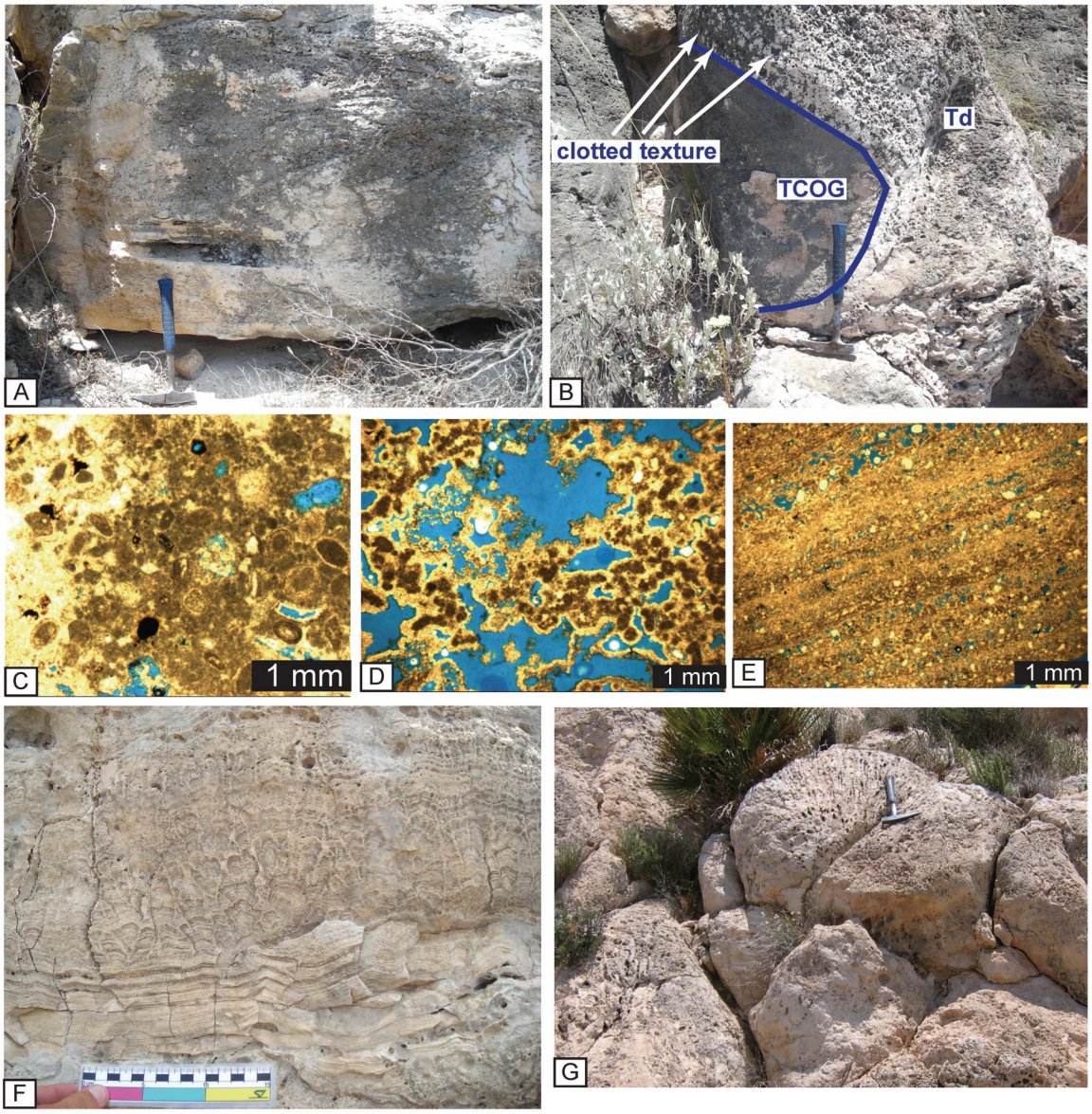

Figure 10: Lithofacies photographs and photomicrographs. Hammer is 32 cm long and field scale is marked in centimeter increments with black and white bars. Scales for photomicrographs are in the right corner and are 1 mm. A. Photograph of the trough cross-bedded ooid bivalve grainstone (TCOBG) characterized by abundance of bivalves showing meter-scale troughs. B. Photograph of the thrombolite boundstone lithofacies. This photo shows the thrombolite boundstone interbedded with TCOG in Sequence 2 on the west side of La Molata. Dark clots and the morphology allow for identification. C. Photomicrograph of a dense thrombolite boundstone (Td) showing peloids and ooids within the peloidal clotted matrix. D. Photomicrograph of a vuggy thrombolite (Tv) showing the clotted texture and great abundance of vugs. E. Photomicrograph of the stromatolite lithofacies showing fine laminae alternating with coarse laminae consisting of common volcaniclastic grains and fenestrae. F. Photograph of finely planar laminar stromatolite of Sequence 4 becoming digitate upward. G. Photograph of the *Porites* boundstone lithofacies taken from the lowest elevations of La Rellana where the lithofacies is laterally extensive and thick. Massive coral heads consisting dominantly of *Porites* commonly range from 1-3 m wide and 2-3 m thick.

of the near-shore environment.

Thrombolite boundstone

The thrombolite boundstone (Table 1; Appendix IX) ranges in thickness from 0.27-5 m, with thickest accumulations occurring at low elevations. It is present in Sequences 1, 2, 3, and 4 at La Molata and Sequences 2 and 4 at La Rellana/Ricardillo. This lithofacies is subdivided into two subfacies on the basis of texture: 1) dense thrombolite boundstone (Td), characterized by approximately < 15 percent vugs; and 2) vuggy thrombolite boundstone (Tv), characterized by approximately > 15 percent vugs. There has yet to be a rationale identified for why and where vugs are more abundant, so for the purpose of this study the Td and Tv are lumped together for stratigraphic documentation in later portions of this report. The thrombolite boundstone lithofacies builds topographic relief. At the low elevations, the lithofacies is laterally extensive (6 m to up to 10s of m) and thickest (up to 5 m) stratigraphically low in the sequences. At the lowest elevations, the thrombolite boundstone is locally laterally extensive (<1 m up to 10s of m) and is <2 m in thickness stratigraphically high in the sequences. At high elevations, the lithofacies becomes isolated bioherms (1-2 m wide) and thinner (commonly <2 m). A dark clotted texture characterizes this lithofacies; it is observable in the field and confirmed as clotted (peloids) texture in thin section (Figure 10B, C, D). This lithofacies consists of varying amounts of gastropod, bivalve, serpulid worm fragments, calcareous red algae, benthic forams, ooids, and peloids; rare volcaniclastic grains, *Porites, Tarbellastrea,* and solitary corals occur. Corals occur only in Sequence 3. Calcareous red algae are more abundant in thrombolite boundstone of Sequence 2 at La

Molata. Serpulid worm fragments are most abundant in the thrombolite boundstone of Sequence 4.

Interpretation

Previous studies on thrombolites, and similarly termed microbialites, worldwide and across many geologic time periods, have interpreted them to be deposited over a vast variety of depths. Interpreted depths of formation have proven hard to constrain, with estimates ranging from relatively deep waters (between 50-200 m) to shallow water depths (< 10 m), (Braga et al., 1995; Mancini et al., 1998; Grotzinger et al., 2000; Mancini and Parcell, 2001; Whalen et al. 2002; Adams et al., 2004; Batten et al., 2004; Mancini et al., 2004; Adams et al., 2005; Heydari and Baria, 2005; Mancini et al., 2008; Planavsky and Ginsburg, 2009).

For my study, the occurrence of thrombolite boundstones in association with other lithofacies provides some constraints. Where thrombolite boundstone is interbedded with the ooid grainstones, a depth of less than 10 m is interpreted. Other occurrences are more difficult to constrain, such as where thrombolite boundstone is stratigraphically low in sequences. In these occurrences, the inclusion of miliolid forams and ooids in the clotted matrix suggests nearby shallow water environments. In addition, the association of many thrombolite boundstones with high energy lithofacies, such as trough cross-bedded ooid grainstone, trough cross-bedded ooid bivalve grainstone, and cross-bedded oolitic gastropod grainstone, suggests a high energy environment for the thrombolites. The diverse faunal assemblage included in many of the thrombolite boundstones indicates relatively normal marine conditions.

Stromatolite

The stromatolite lithofacies (Table 1; Appendix IX) ranges from 0.05-0.7 m in thickness and is almost exclusively deposited as the basal lithofacies of sequences. Stromatolites also occur within the *Porites* boundstone lithofacies and are rarely found within the thrombolite boundstone lithofacies. The lithofacies is very finely laminated with a peloidal and clotted texture (Figure 10E). The lamination commonly alternates with finer and coarser grains. Stromatolites predominantly consist of abundant micrite and peloids with common volcaniclastic grains; rarely, ooids are the dominant grain type. At high elevations in Sequence 2, the stromatolites are thicker (0.2-0.7 m) and consist of abundant ooid grains. In Sequence 4, the stromatolites become digitate in morphology stratigraphically higher in the section (Figure 10F).

Interpretation

Stromatolite morphology is affected primarily by environmental factors such as water depth, current energy, sediment influx, and lithification (Grotzinger and Knoll, 1999). The fine planar laminations, abundance of peloids, micrite, and volcaniclastic grains, indicates the finely planar laminated micritic peloidal stromatolite was deposited in shallow water (<10 m), low energy environments (Hoffman, 1976). The planar laminations, abundance of ooids, peloids, micrite, and volcaniclastic grains indicates the planar laminated oolitic stromatolite was deposited in shallow water (<10 m) with moderate to high energy (Hoffman, 1976). The change from fine planar laminated stromatolite to digitate stromatolite is interpreted to show a change to higher energy environment of deposition and possible increase of accommodation space (Hoffman,

1976). The lack of fauna and preservation of the stromatolites possibly indicates restricted marine conditions.

Porites boundstone

The *Porites* boundstone (Table 1; Appendix IX) is only found in Sequence 3 at both locations. At La Molata, the lithofacies occurs as rare, small (generally 1-2 m wide and 2 m thick), in-growth or out-of-growth position patch reefs. At La Rellana/Ricardillo, the lithofacies occurs as in-growth position patch reefs generally 1-2 m wide and 2-3 m thick; at the lowest elevations (181-200 m) the reefs are laterally extensive (up to >10 m) and thick (up to 6 m) (Figure 10G). The lithofacies consists of framework-forming *Porites* and *Tarbellastrea* corals with stick, knobby, and laminar morphology, varying amounts of gastropods, bivalves, serpulid worms, calcareous red algae (encrusting, fragments, rhodoliths), stromatolite, clionid sponges, ooids, peloids, and micrite.

Interpretation

The upper Miocene reefs have been extensively studied throughout the Mediterranean (Esteban et al., 1978; Esteban, 1979; Esteban and Giner, 1980; Dabrio et al., 1981; Franseen and Mankiewiz, 1991; Martin and Braga, 1994; Goldstein and Franseen, 1995; Esteban, 1996; Esteban et al., 1996; Franseen and Goldstein, 1996; Toomey, 2003). Zonations within the colonial morphologies of the reefs have been proposed by Esteban (1996) with encrusting morphologies dominating in <10 m water depth, stick morphologies dominating 10-20 m water depth, and laminar morphologies dominating 20-30 m water depth. Observations from my study area are inconsistent with this depth zonation. Laminar and stick morphologies of *Porites* are interbedded with in-

place trough cross-bedded ooid grainstone, suggesting deposition in <10 m water depth. The *Porites* morphologies, ooids, and interbedding with trough cross-bedded ooid grainstone indicate that the *Porites* boundstone lithofacies was deposited in shallow waters (<10 m) with high energy conditions. The diverse fauna assemblage suggests relatively normal marine conditions during deposition.

STRATIGRAPHY

The generalized stratigraphy for the La Molata and La Rellana/Ricardillo field areas was introduced in the lithofacies section with Figures 5 and 6. The following text examines stratigraphic relationships in more detail for each field area.

La Molata TCC Stratigraphy

Figure 11 is a fence diagram showing stratigraphic relationships and lithofacies distribution throughout the La Molata field area. A cross-section of La Molata's north side is used as representative for the area (Figure 12).

Sequence 1

Sequence 1 extends for 0.6 km in the La Molata field area and is absent on the western margin. The sequence ranges in thickness from 1.35–8.5 m and drapes paleotopography. Master beds within the sequence gently dip to the west, south, and east at 2–5 degrees, away from the central high.

The lowest elevations (170-180 m) have local laterally extensive stromatolites overlain by local laterally extensive thrombolite boundstone that is interbedded with, and subsequently overlain by trough cross-bedded ooid grainstone (Figure 13). Where the

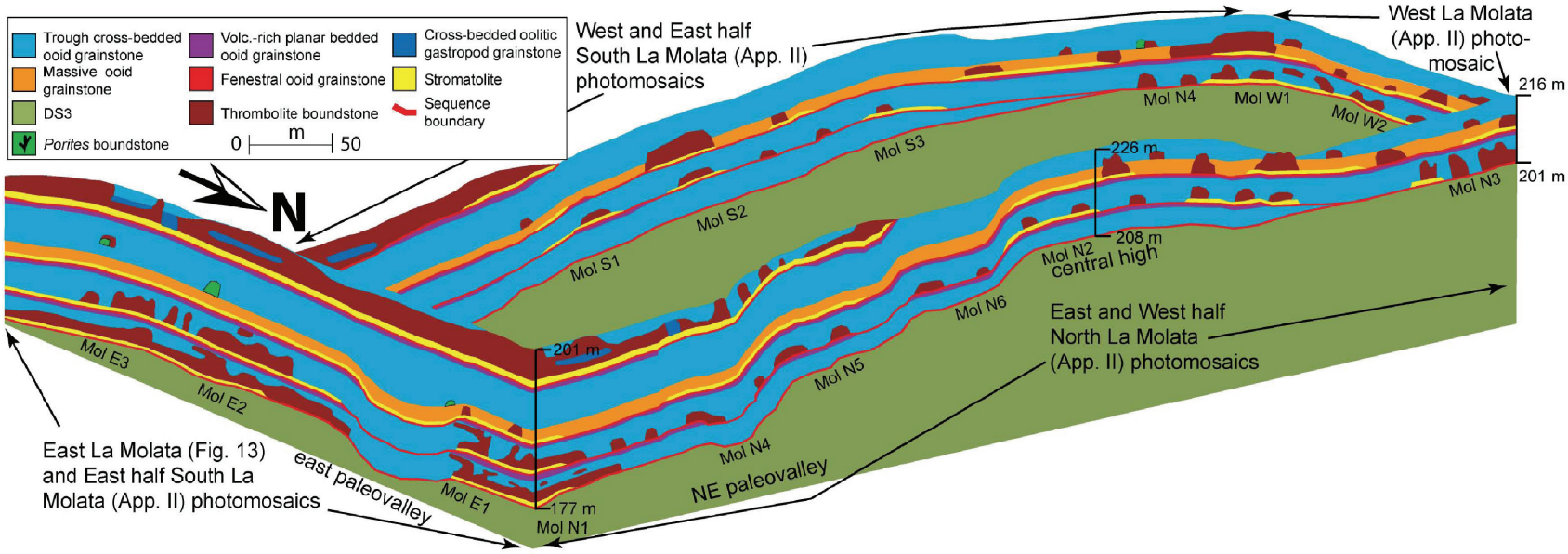

Figure 11: Fence diagram for the La Molata Field area displaying the distribution and geometries of lithofacies. Sequences drape and locally onlap paleotopography and maintain relatively uniform thickness across the area. Oolites are volumetrically the most abundant lithofacies. Thrombolite boundstones are laterally extensive and thicker at the low elevations. Stromatolites are laterally more extensive at the low elevations.

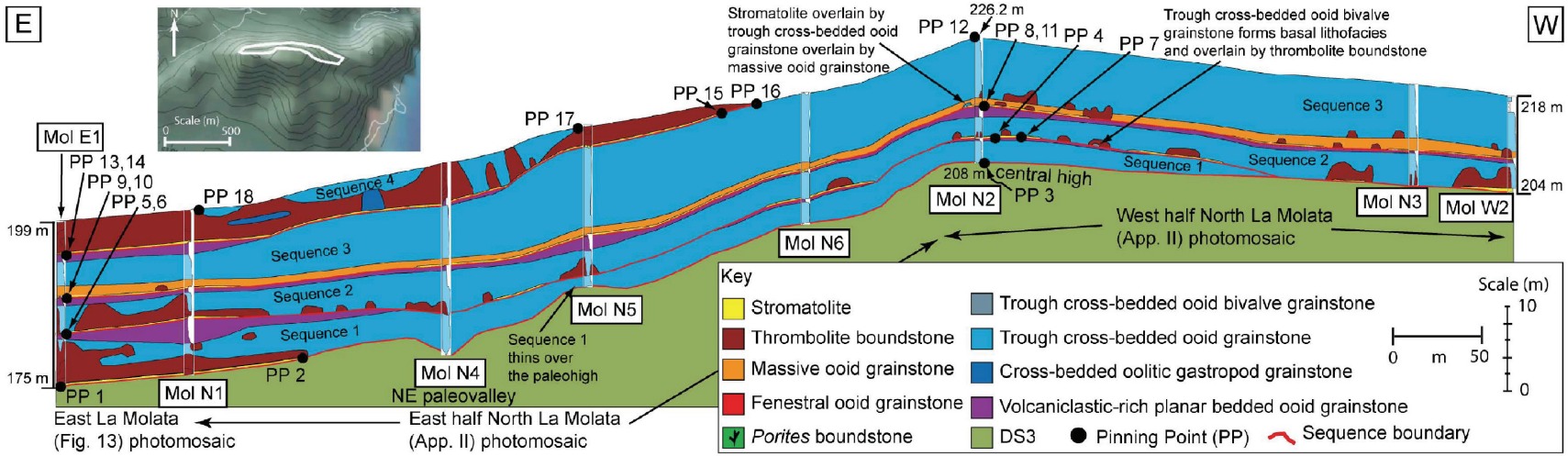

Figure 12: Cross-section of the north side of the La Molata field area. Pinning points (PP) are used to construct the relative sea-level curve of Figure 19. Thrombolite boundstones build topographic relief stratigraphically lower in the section during relative sea-level rises. Oolites fill in topographic relief during the relative falls in sea-level. The central high persisted as the highest elevation throughout TCC deposition. Notice the heterogeneity caused by complex lithofacies distribution and geometries.

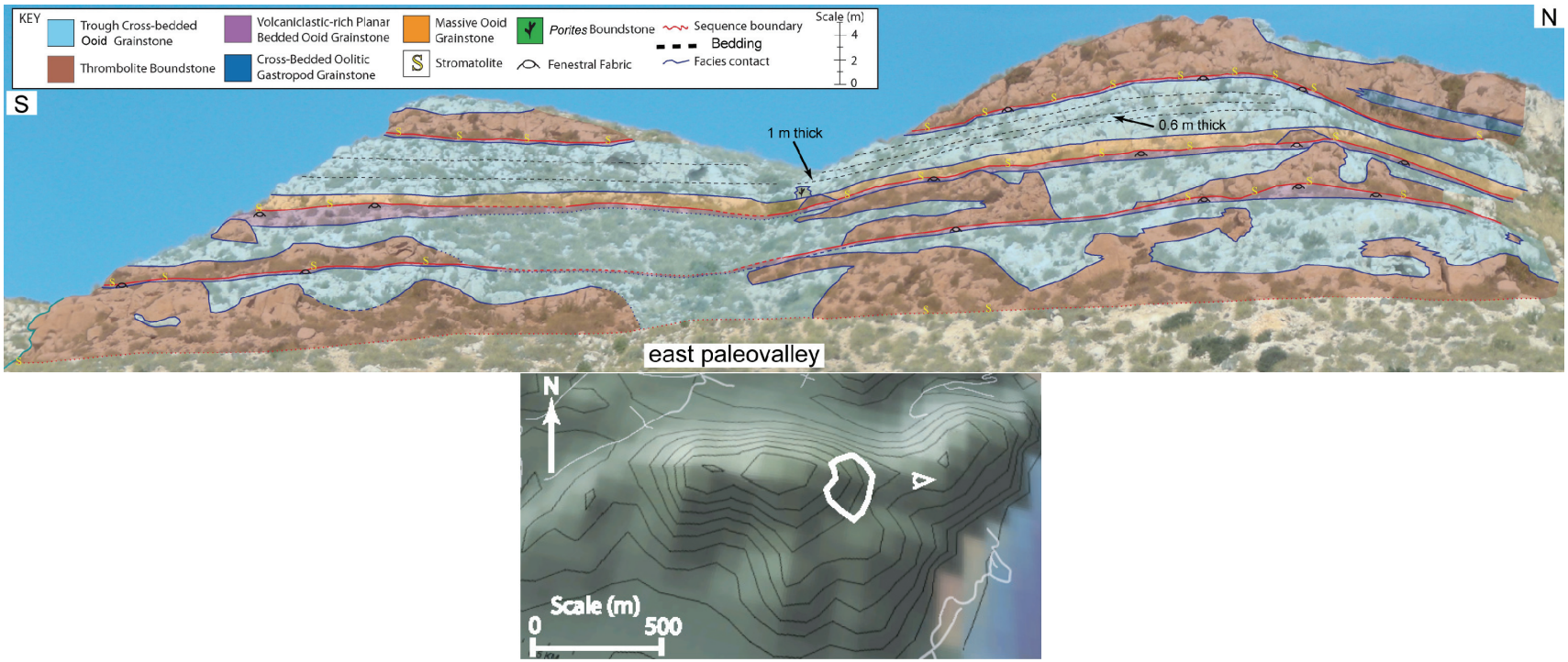

Figure 13: Photomosaic of the east side of La Molata. Thrombolite boundstone is interbedded with trough cross-bedded ooid grainstone stratigraphically high in the section of Sequences 1 and 2. The thrombolites stratigraphically higher in the sequences accumulate more laterally than vertically as compared to the thrombolites stratigraphically lower in the sequences. Bedding in Sequence 3 is shown with beds becoming thicker and dipping towards the center of the east paleovalley.

stromatolites and thrombolite boundstones are absent, trough cross-bedded ooid grainstone forms the basal lithofacies. The trough cross-bedded ooid grainstone grades upward locally to volcaniclastic-rich planar bedded ooid grainstone and the sequence is capped in places by fenestral ooid grainstone. At elevations above 180 m, trough cross-bedded ooid grainstone forms the basal lithofacies; it grades upward to volcaniclastic-rich planar bedded ooid grainstone locally, and the sequence is capped in places by fenestral ooid grainstone.

Sequence 2

Sequence 2 is present in its entirety over all of the paleotopographic elements of the La Molata field area. The sequence ranges in thickness from 3.9–7.1 m, and as a package, drapes the paleotopography. Master beds gently dip away from the central high to the west, south, and east at 2–5 degrees with higher dips on the southern end of the western margin that range between 15–23 degrees to the southeast.

The low elevations (170-190 m) of Sequence 2 have locally laterally extensive stromatolites overlain by local thrombolite boundstone that becomes interbedded with, and subsequently overlain by trough cross-bedded ooid grainstone. Where stromatolites and thrombolite boundstone are absent, trough cross-bedded ooid grainstone forms the basal lithofacies. The trough cross-bedded ooid grainstone grades upward locally to volcaniclastic-rich planar bedded ooid grainstone, and the sequence is capped in places by fenestral ooid grainstone. The thrombolite boundstones are thickest (up to 5 m) and laterally extensive (up to 10's of m) at the lowest elevations (170-180 m, Figure 13) and become more isolated (generally <3 m wide and <2 m thick) above 180m. The high

elevations (190-208 m) of Sequence 2 have local stromatolites overlain by local isolated (1-2 m wide and 1-3 m thick) thrombolite boundstone overlain by trough cross-bedded ooid grainstone. The trough cross-bedded ooid grainstone locally grades upward to volcaniclastic-rich planar bedded ooid grainstone, and the sequence is capped in places by fenestral ooid grainstone. A small area just west of the central high has trough cross-bedded ooid bivalve grainstone (1 m laterally and < 1 m in thickness) overlain by thrombolite boundstone at the base of the cycle (Figure 12). The western margin of La Molata (201–204 m) has thrombolite boundstone stratigraphically higher in the sequence that is interbedded with trough cross-bedded ooid grainstone.

Sequence 3

Sequence 3 is present over the entire La Molata field area. The sequence ranges in thickness from 6.3–12.8 m and as a package drapes paleotopography. Master beds gently dip to the west, south, and east from the central high at 2–5 degrees, with higher dips on the southern end of the western margin at 8–15 degrees to the southeast.

The low elevations (170-190 m) of Sequence 3 have local laterally extensive stromatolites overlain by massive ooid grainstone. Rare, isolated (1 m wide and 1 m thick) thrombolite boundstone locally overlies the stromatolites and exhibits a sharp contact with the massive ooid grainstone above and on the sides. The massive ooid grainstone grades upward to trough cross-bedded ooid grainstone that locally grades upward to volcaniclastic-rich planar bedded ooid grainstone. The sequence is capped in places by fenestral ooid grainstone. Rare, isolated (0.5-2 m wide and 0.5-3 m thick) *Porites* boundstone patch reefs are interbedded within the trough cross-bedded ooid

grainstone and rarely overlain by thrombolite boundstone. The high elevations (190-208 m) for Sequence 3 have local laterally extensive stromatolites overlain by massive ooid grainstone that is interbedded with, and locally overlain by, thrombolite boundstone. The contact between the massive ooid grainstone and thrombolite boundstone can be sharp or gradational. The massive ooid grainstone grades upward to trough cross-bedded ooid grainstone. The trough cross-bedded ooid grainstone is interbedded with local thrombolite boundstone stratigraphically lower in the sequence. Rare, isolated (1 m wide and 1 m thick) *Porites* boundstone patch reefs are interbedded with the trough cross-bedded ooid grainstone and are rarely overlain by thrombolite boundstone. On the eastern side of the central high, basal stromatolite is locally overlain by trough cross-bedded ooid grainstone that is overlain by massive ooid grainstone; details are limited because of poor outcrop exposure (Figure 12).

Sequence 4

Sequence 4 is preserved as an erosional remnant only along 0.22 km of outcrop trace (170–197 m in elevation) on the eastern portion of La Molata. The sequence ranges in thickness from 1.7–6.2 m (6.2 m is upper thickness limit due to modern erosion) and as a package drapes paleotopography.

Sequence 4 has basal stromatolite overlain by thrombolite boundstone interbedded with cross-bedded oolitic gastropod grainstone that is overlain by trough cross-bedded ooid grainstone (Figure 13). The contact between the cross-bedded oolitic gastropod grainstone and thrombolite boundstone is gradational.

La Rellana/Ricardillo TCC Stratigraphy

Figure 14 is a fence diagram showing the stratigraphic relationships and distribution of lithofacies throughout the La Rellana/Ricardillo field area. Figure 15 is a representative cross-section of the La Rellana/Ricardillo field area.

Sequence 1

Sequence 1 at La Rellana/Ricardillo is preserved along 2.65 km of linear outcrop in the field area; it is absent on the eastern margin of Cerro de Ricardillo. The sequence ranges in thickness from 1.6–5.9 m and drapes paleotopography. In general, master beds within the sequence dip gently (1 – 11 degrees) to the south-southeast (towards the modern Mediterranean Sea) with local variations due to paleotopography (Appendix X).

Throughout its exposure, Sequence 1 has bioturbate ooid grainstone that gradationally transitions upward and laterally updip to trough cross-bedded ooid grainstone. The trough cross-bedded ooid grainstone gradationally transitions upward and laterally updip to planar-bedded ooid grainstone. Planar-bedded ooid grainstone locally grades upward to volcaniclastic-rich planar bedded ooid grainstone, and the sequence is capped in places by fenestral ooid grainstone. Rarely the planar bedded ooid grainstone or bioturbate ooid grainstone lithofacies is absent.

Sequence 2

Sequence 2 traces across the entirety of the La Rellana/Ricardillo field area (181–257 m of elevation). The sequence ranges in thickness from 1.2–5.9 m (5.9 is a minimal upper limit to thickness due to erosion after deposition) and drapes paleotopography.

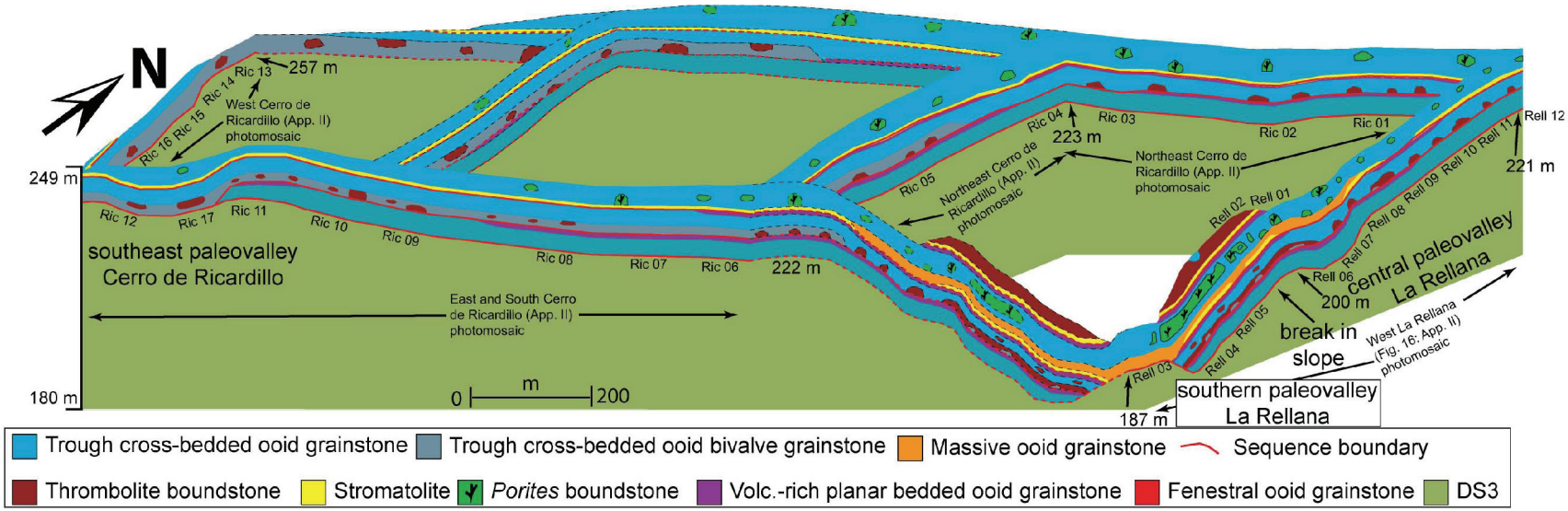

Figure 14: Fence diagram for the La Rellana/Ricardillo field area displaying the distribution and geometries of lithofacies. Sequences drape paleotopography and maintain relatively uniform thickness across the area with oolite lithofacies dominant. *Porites* boundstone in Sequence 3 is laterally extensive and thick at the lowest elevations and is much more abundant throughout the field area compared to La Molata. No stromatolites occur in Sequences 1 and 2 of La Rellana/Ricardillo.

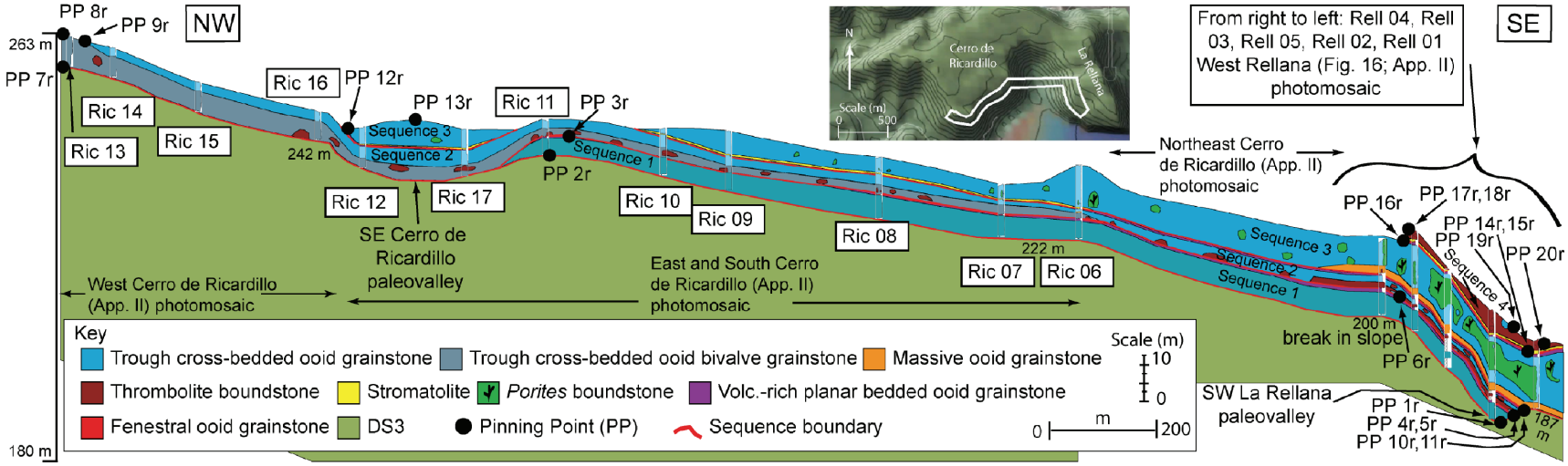

Figure 15: Cross-section of the La Rellana-Ricardillo field area. Pinning points (PP) are used to construct the sea level curve of Figure 20. Thrombolite boundstone is thicker and laterally extensive at the lower elevations and becomes isolated at higher elevations in Sequence 2. At the lowest elevations, the thrombolite boundstones are interbedded with trough cross-bedded ooid grainstone stratigraphically higher in Sequence 2. *Porites* boundstone in Sequence 3 is laterally extensive and thick at the lowest elevations downdip of a pronounced break in slope. Massive ooid grainstone occurs only in Sequence 3 below 217 m substrate elevation.

Master beds appear to generally dip gently (2-9 degrees) to the south with local variations due to paleotopographic highs and lows.

The low elevations (181-221 m) have local thrombolite boundstone overlain by trough cross-bedded ooid grainstone. The trough cross-bedded ooid grainstone locally grades upward to volcaniclastic-rich planar bedded ooid grainstone, and the sequence is capped in places by fenestral ooid grainstone. At the lowest elevations (181-200 m), the thrombolite boundstone is laterally extensive and interbedded with trough cross-bedded ooid grainstone stratigraphically higher in the sequence (Figure 16). Rare, isolated (<0.5 m in thickness and <2 m laterally) trough cross-bedded ooid bivalve grainstone accumulations overlain by thrombolite boundstone form the basal lithofacies for the sequence. The high elevations (221-257 m) of Sequence 2 have trough cross-bedded ooid bivalve grainstone interbedded with thrombolite boundstone and overlain by trough cross-bedded ooid grainstone. The contact between the trough cross-bedded ooid bivalve grainstone and trough cross-bedded ooid grainstone is commonly sharp, but locally gradational. The trough cross-bedded ooid grainstone locally grades upward to volcaniclastic-rich planar bedded ooid grainstone, and the sequence is capped in places by fenestral ooid grainstone. Only trough cross-bedded ooid bivalve grainstone (thicker than at lower elevations) and rare thrombolite boundstone are found at the highest elevations (242-257 m).

Sequence 3

Sequence 3 is preserved across the entire La Rellana/Ricardillo field area, except at the highest elevations (240–257 m). The sequence ranges in thickness from 10.3–11.8

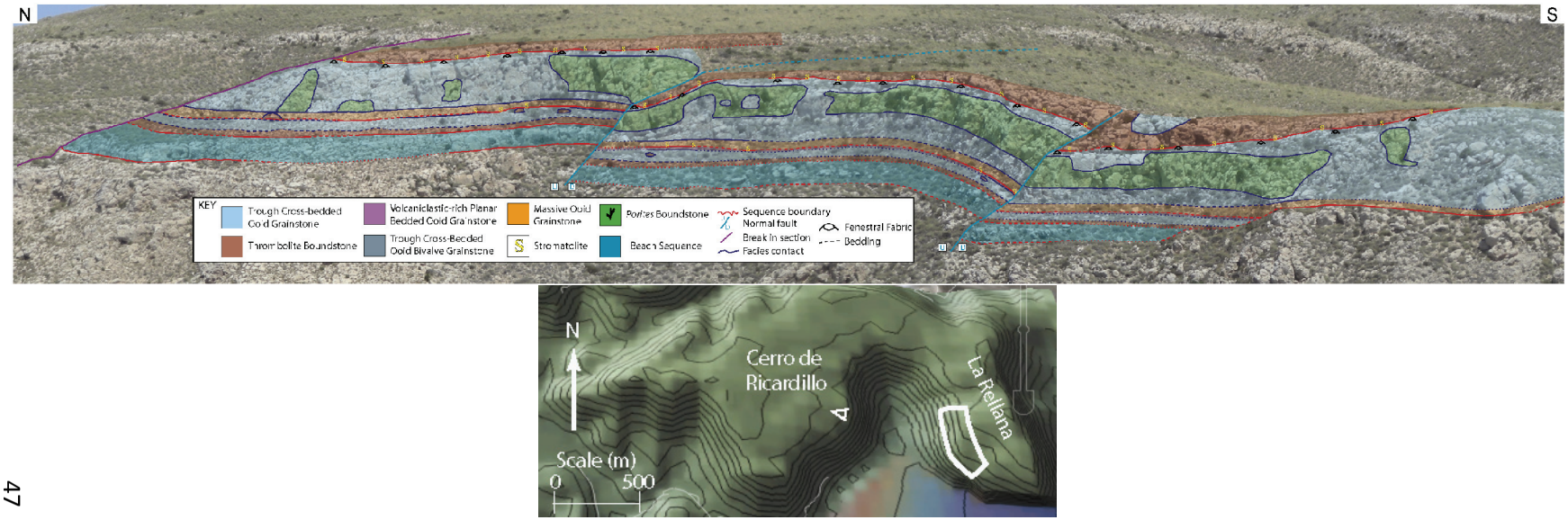

Figure 16: Photomosaic of the southern margin of La Rellana. Thrombolite boundstones are laterally extensive and are interbedded with trough cross-bedded ooid grainstone stratigraphically higher in Sequence 2. Sequence 3 has massive ooid grainstone above the stromatolite lithofacies and *Porites* boundstone is laterally extensive and thick at this location. Sequences 1 and 2 deposits lap-out against reef core deposits of DS3 in the southern paleovalley.

m where fully preserved and 1.1–10.3 m where partially preserved due to modern erosion; this sequence drapes paleotopography. Although difficult to identify, master beds generally dip gently (2-9 degrees) to the south with local variations due to paleotopography.

The low elevations (181-217 m) of Sequence 3 have local laterally extensive stromatolites overlain by massive ooid grainstone that grade upward to trough cross-bedded ooid grainstone interbedded with *Porites* boundstone. At the lowest elevations (181-200 m), the *Porites* boundstone is thick (up to 6 m) and laterally extensive (10s of m). At these elevations the trough cross-bedded ooid grainstone grades upward to volcaniclastic-rich planar bedded ooid grainstone; in places, fenestral ooid grainstone caps the sequence (Figure 16). Above 200 m elevation, the *Porites* boundstone lithofacies occurs as isolated patches (generally <3 m thick and <2 m wide). The high elevations (217-240 m) of Sequence 3 have laterally extensive stromatolites overlain by trough cross-bedded ooid grainstone interbedded with isolated *Porites* boundstone patches.

Sequence 4

Sequence 4 crops out along a lateral exposure of 0.3 km, and is absent above 200 m. The sequence ranges in thickness from 0.4–5.1 m (5.1 being a minimal maximum thickness due to modern erosion). As a package, it drapes paleotopography. Sequence 4 has basal stromatolites overlain by thrombolite boundstone that is overlain rarely by trough cross-bedded ooid grainstone (Figure 16).

DEPOSITIONAL CONTROLS

Similar stratigraphy at similar elevations, between the two areas, suggests that sea level and paleotopography are the primary controls. The stratigraphic differences between the two areas show how local paleogeography and currents have a secondary effect.

Relative Sea Level

The four TCC sequences that were deposited at both field locations of this study have been interpreted in previous studies to result from relative rises and falls in sea level (Franseen and Mankiewicz, 1991; Franseen et al., 1993; Goldstein and Franseen, 1995; Whitesell, 1995; Franseen et al., 1997a; Franseen et al. 1998; Franseen and Goldstein, 2004; Franseen and Goldstein, 2007)). In addition to these studies, and the results of my work, similar types and number of sequences have been documented by other authors in the TCC of southeast Spain (Esteban and Giner, 1980; Valles Roca, 1986; Braga and Martin, 1992; Calvet et al., 1996; Esteban et al., 1996) and TCC-like deposits of approximately the same age documented around the entire Mediterranean basin (Valles Roca, 1986; Cunningham 1995; Calvet et al. 1996; Esteban 1996; Esteban et al., 1996), which suggests at least a regional control for sequence development. Furthermore, paleomagnetic data collected by Franseen et al. (1998) correlated the four TCC sequence boundaries to a similar number of subaerial exposure surfaces at Niue in the South Pacific (Lu et al., 1996), suggesting a possible global control on sea-level change responsible for TCC cycles.

Quantitative relative sea-level curves were created for both field areas using the pinning point method of Goldstein and Franseen (1995). Those authors define a pinning

point "as a point of quantitative constraint on the position of ancient sea level relative to an arbitrarily defined geologically useful starting elevation." For the purposes of this study, modern substrate elevations are used as the geologically useful starting elevation, as paleotopography has been shown to be largely preserved for the areas, and modern relative elevation differences would largely represent relative differences in the elevation of Messinian sea-level positions. Lithofacies and features indicative of the position of sea level (pinning points) and the ability to trace these lithofacies across paleotopography provided the basis for construction of the sea-level curves for La Molata (Figure 17) and La Rellana/Ricardillo (Figure 18). Straight lines were used between pinning points as the simplest representation of sea level between data points. Curves are left open between rises and falls where there was no evidence that sea level turned around at these points. The majority of pinning points were placed where marine inundation of subaerial exposure and subaerial exposure of marine rocks occurred. Trough cross-bedded oolite lithofacies, deposited in depths of less than 10 m, were used to indicate ancient sea-level position with an error bar of 10 m. Certain pinning points are designated at an upslope or downslope outcrop limit as evidence that sea level must have passed by the location. The data used to construct the sea-level curves and each pinning point for the two areas is explained below.

La Molata Sea Level History

Figure 12 shows a cross-section of La Molata with each pinning point that was used to construct the sea-level curve in Figure 17.

- Pinning point 1 is located at 175 m substrate elevations where stromatolite was deposited over the subaerial exposure surface (SB5) on DS3.

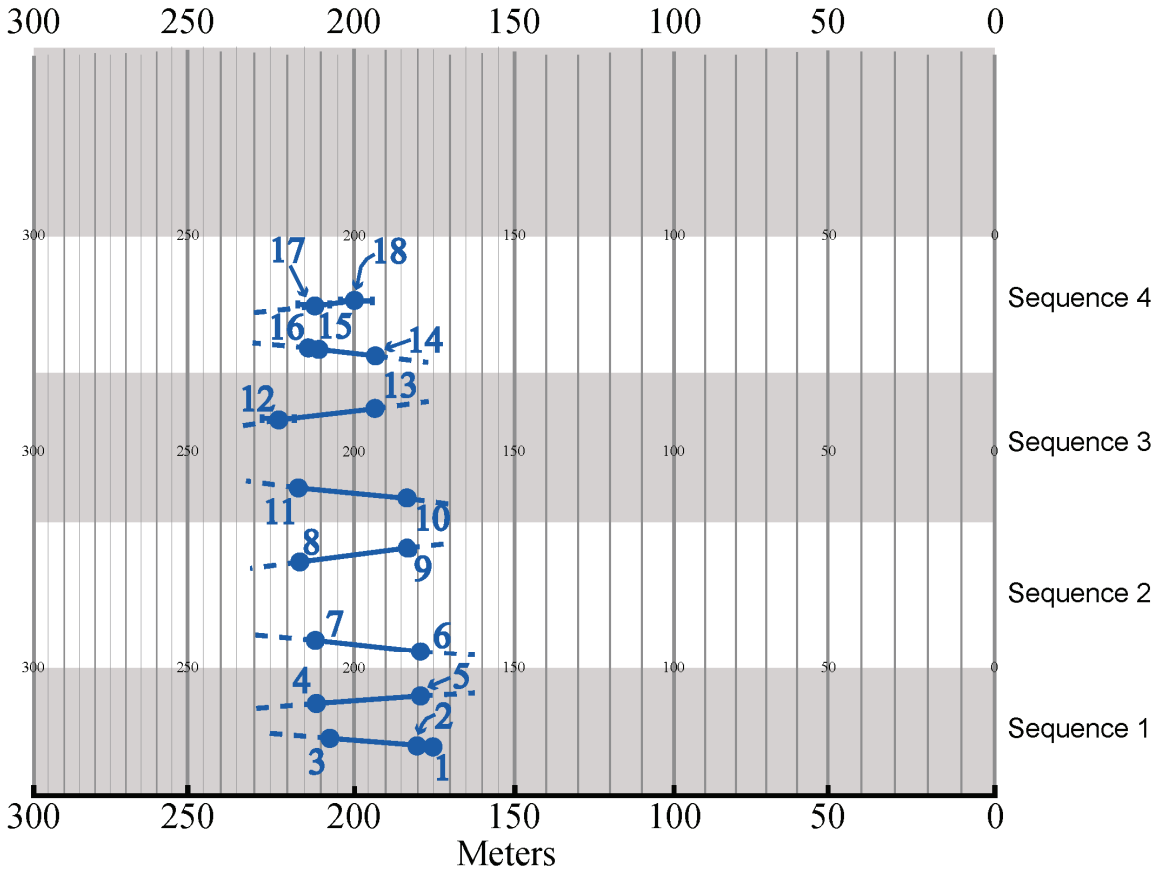

Figure 17: Quantitative relative sea-level curve for the La Molata field area based on pinning points. See Figure 12 for location of pinning points. Sea-level fluctuations for La Molata range between 32.3 and 43.1 m.

- Pinning point 2 represents a sea-level rise of 5 m with deposition of stromatolite over subaerial exposure surface on DS3 at 180 m substrate elevation.
- Pinning point 3 represents continued sea-level rise of 28 m from pinning point 2 and is located at the base of trough cross-bedded ooid grainstone deposited on the subaerial exposure surface of DS3 at 208 m substrate elevation. This represents the highest marine sedimentations of Sequence 1 over the highest exposure surface on DS3 and marks a location that sea level must have passed.
- Sea level continued to rise with the deposition of thrombolite boundstone at the lowest elevations of 175–180 m (Figure 13). Due to lack of depth constraints for thrombolite boundstone deposition during sea-level rises, no pinning points are indicated.
- Sea level rose to an unknown elevation and then began to fall.
- Pinning point 4 represents the highest preserved sea-level position for Sequence 1 at La Molata with fenestral ooid grainstone capping volcaniclastic-rich planar bedded ooid grainstone on the central high at 211.5 m substrate elevation. This pinning point is designated on the relative fall in sea level because it represents sequence-capping subaerial exposure.
- Sea level continued to fall and thrombolite boundstone deposition either continued or was reinitiated, typically atop of previous deposits of thrombolite boundstone that likely provided a hard substrate for subsequent thrombolite boundstone deposition, at the lowest elevations (175 – 180 m).

- Pinning point 5 occurs where a fenestral ooid grainstone caps volcaniclastic-rich planar bedded ooid grainstone at 179.2 m elevation representing a sea-level fall of at least 32.3 m from pinning point 4. This is the last preserved deposition of Sequence 1.
- Sea level fell to an unknown elevation and then began to rise.
- Pinning point 6 is indicated by stromatolites of Sequence 2 overlying fenestral ooid grainstone of Sequence 1 at 179.2 m elevation, which represents a relative sea-level rise.
- Pinning point 7 is indicated by oolitic stromatolites of Sequence 2 overlying fenestral ooid grainstone of Sequence 1 on the central high at 211.8 m substrate elevation and represents 32 m of sea-level rise from pinning point 6.
- Sea level rose to an unknown elevation and then began to fall.
- Pinning point 8 represents the highest preserved sea-level position of Sequence 2 at La Molata where fenestral ooid grainstone caps volcaniclastic-rich planar bedded ooid grainstone on the central high at 216.3 m substrate elevation. This pinning point is designated on the relative fall in sea level and not the continued rise in sea level.
- Pinning point 9 is indicated by fenestral ooid grainstone capping volcaniclastic-rich planar bedded ooid grainstone at 183.1 m substrate elevation, which represents a minimum sea-level fall of 33.2 m from pinning point 8 and the last preserved deposition of Sequence 2.
- Sea level fell to an unknown elevation and then began to rise.
- Pinning point 10 is indicated by stromatolites of Sequence 3 overlying fenestral ooid grainstone of Sequence 2 at 183.1 m substrate elevation, which represents a sea-level rise.

- Pinning point 11 is indicated by stromatolite deposition at 216.3 m substrate elevation on the central high, immediately above fenestral ooid grainstone of Sequence 2, which represents a continued sea-level rise of 33.2 m from pinning point 10.
- Sea level rose to an unknown elevation and then began to fall.
- Pinning point 12 represents the highest sea-level position preserved for Sequence 3 at La Molata where erosionally truncated trough cross-bedded ooid grainstone represents shallow water during time of deposition on the central high at 226.2 m substrate elevation. The entire sequence is not preserved here likely due to modern erosion. This pinning point is designated on the relative fall in sea level and not the continued rise in sea level.
- Pinning point 13 is indicated by fenestral ooid grainstone capping volcaniclastic-rich planar bedded ooid grainstone at 193.1 m substrate elevation, which represents a minimum sea-level fall of 33.1 m from pinning point 12 and the last preserved deposition of Sequence 3.
- Sea level fell to an unknown elevation and then began to rise.
- Pinning point 14 represents a sea-level rise with stromatolites of Sequence 4 overlying fenestral ooid grainstone of Sequence 3 at 193.1 m substrate elevation.
- Pinning point 15 represents a continued sea-level rise of 17.3 m from pinning point 14 with stromatolites of Sequence 4 overlying trough cross-bedded ooid grainstone of Sequence 3 at 210.4 m substrate elevation.
- Pinning point 16 represents continued sea-level rise of 3.3 m from pinning point 15 where thrombolite boundstone of Sequence 4 overlies trough cross-bedded ooid

grainstone of Sequence 3 at 213.7 m substrate elevation at the updip extent for sequence deposition in this area.

- Sea level rose to an unknown elevation and began to fall.
- Pinning point 17 represents a sea-level fall with erosionally truncated trough cross-bedded ooid grainstone at 212 m substrate elevation. This pinning point is designated on the relative fall in sea level and not the continued rise.
- Pinning point 18 is indicated by erosionally truncated trough cross-bedded ooid grainstone at 200 m substrate elevation, which represents a continued sea-level fall of 12 m from pinning point 17.

La Rellana/Ricardillo Sea Level History

Figure 15 shows a cross-section of La Rellana/Ricardillo with each pinning point that was used to construct the relative sea-level curve in Figure 18.

- Pinning point 1r is located at 181 m substrate elevation at the base of the bioturbate ooid grainstone deposited on top of the subaerial exposure surface (SB5) on DS3. This is the lowest elevation that initial TCC deposits are found and means that sea level must have passed this point.

- Pinning point 2r is located at 239 m substrate elevation at the base of the bioturbate ooid grainstone deposited over SB5. Sea level must have passed this point during the rise and represents 58 m of rise from pinning point 1r.

- Sea level rose to an unknown elevation and began to fall.

- Pinning point 3r is located at 242.4 m substrate elevation and is the highest preservation of Sequence 1 in the area. Paleotopography drops and then rises to the

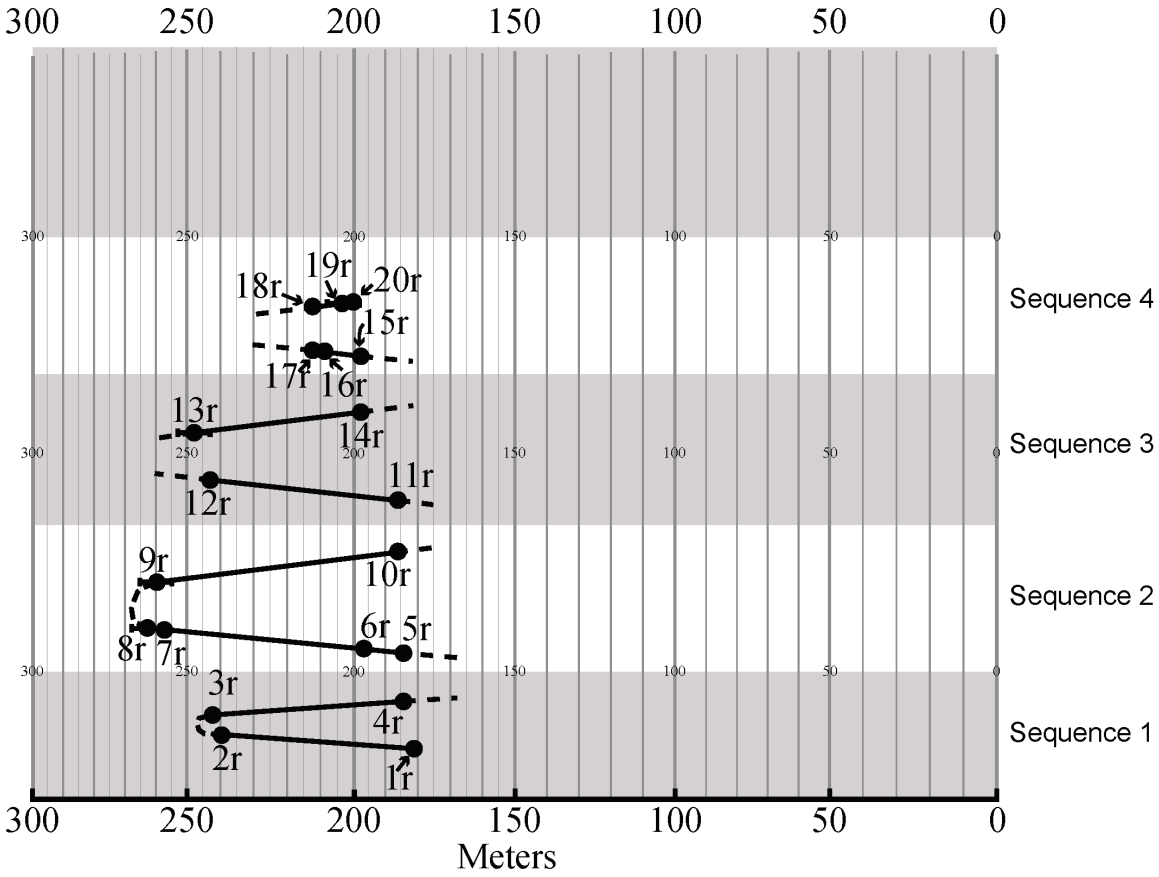

Figure 18: Quantitative relative sea-level curve for the La Rellana/Ricardillo field area based on pinning points. See Figure 15 for location of pinning points. La Rellana/Ricardillo field area reaches higher elevations and thus recorded greater amplitudes of sea-level fluctuation. Minima for amplitudes ranged between 57.8 and 76.6 m.

west of this location, but Sequence 1 is not preserved west of this point possibly due to past subaerial exposure between sequences. The pinning point is indicated by fenestral ooid grainstone capping volcaniclastic-rich planar bedded ooid grainstone and represents a minimum sea-level rise of 3.4 m from pinning point 2r. Pinning points 2r and 3r are connected by a curved dashed line because no evidence was present in the rock record suggesting that sea level rose significantly higher.

- Pinning point 4r is indicated by fenestral ooid grainstone capping volcaniclastic-rich planar bedded ooid grainstone located at 184.6 m substrate elevation and represents a sea-level fall of 57.8 m from pinning point 3r. This is the last preserved deposition of Sequence 1.

- Sea level fell to an unknown elevation and then began to rise.

- Pinning point 5r is located at 184.6 m substrate elevation at the base of thrombolite boundstone of Sequence 2, where it overlies fenestral ooid grainstone of Sequence 1. This marks the initial deposition of Sequence 2 and sea level must have passed this point.

- Pinning point 6r is indicated by trough cross-bedded ooid bivalve grainstone deposited at 196.5 m substrate elevation where it overlies fenestral ooid grainstone of Sequence 1 and represents a sea-level rise of 11.9 m from pinning point 5r.

- Pinning point 7r is indicated by trough cross-bedded ooid bivalve grainstone deposited at 257 m substrate elevation where it overlies fenestral ooid grainstone of Sequence 1 and represents a sea-level rise of 60.5 m from pinning point 6r.

- Pinning point 8r is indicated by erosionally truncated trough cross-bedded ooid bivalve grainstone interbedded with thrombolite boundstone at 262.7 m elevation and represents a minimum sea-level rise of 5.7 m from pinning point 7r. This point is located at the updip extent of TCC deposits in the area.

- Pinning point 9r is indicated by erosionally truncated trough cross-bedded ooid grainstone at 259.7 m substrate elevation and represents a minimum sea-level fall of 3 m from pinning point 8r. This location represents the highest elevation of preserved trough cross-bedded ooid grainstone for Sequence 2 and is much thinner than downdip likely due to modern erosion. Pinning points 8r and 9r are connected by a curved dashed line because no evidence was preserved in the rock record suggesting that sea level rose significantly higher. Both the trough cross-bedded ooid bivalve grainstone and trough cross-bedded ooid grainstone are deposited in less than 10 m water depth suggesting sea level did not get any higher than approximately 263 m.

- Pinning point 10r is indicated by fenestral ooid grainstone capping volcaniclastic-rich planar bedded ooid grainstone at 186.1 m substrate elevation and represents a minimum sea-level fall of 73 m from pinning point 9r. This is the last preserved deposition of Sequence 2.

- Sea level fell to an unknown elevation and then began to rise.

- Pinning point 11r is indicated by stromatolites of Sequence 3 deposited over the fenestral ooid grainstone of Sequence 2 at 186.1 substrate elevation and represents a sea-level rise.

- Pinning point 12r is indicated by stromatolites above the underlying fenestral ooid grainstone of Sequence 2 at 242.4 m elevation and represents a minimum sea-level rise of 65.9 m from pinning point 11r.

- Sea level rose to an unknown elevation and then began to fall.

- Pinning point 13r is indicated by erosionally truncated trough cross-bedded ooid grainstone at 246.7 m elevation. This location is the highest preserved elevation for Sequence 3 deposition. Truncation is likely the result of modern erosion. This pinning point is designated on the relative fall in sea level and not the continued rise in sea-level.

- Pinning point 14r is indicated by fenestral ooid grainstone capping volcaniclastic-rich planar bedded ooid grainstone at 197 m elevation and represents a minimum relative sea-level fall of 49.7 m from pinning point 13r. This is the last preserved deposition for Sequence 3.

- Sea level fell to an unknown elevation and then began to rise.

- Pinning point 15r is indicated by stromatolites of Sequence 4 deposited over the fenestral ooid grainstone of Sequence 3 at 197 m substrate elevation and represents a relative sea-level rise.

- Pinning point 16r is indicated by stromatolites deposited at 209.2 m elevation immediately above the underlying sequence boundary, and represents a sea-level rise of 11.7 m from pinning point 15r.

- Pinning point 17r is indicated by thrombolite boundstone of Sequence 4 directly above subaerial exposure surface of Sequence 3 at 211.5 m substrate elevation and represents minimum sea-level rise of 2.3 m from pinning point 15r.
- Sea level rose to an unknown elevation and then began to fall.
- Pinning point 18r is at the same location as pinning point 17r and represents the location that sea level must have passed during the relative fall.
- Pinning point 19r is indicated by erosionally truncated trough cross-bedded ooid grainstone at 204 m elevation and represents a relative sea-level fall of 7.5 m from pinning point 18r.
- Pinning point 20r is indicated by erosionally truncated thrombolite boundstone at 200 m elevation and represents a minimum sea-level fall of 4 m from pinning point 19r. This is the last and lowest elevation of deposition for Sequence 4 in the area and marks the location sea level must have passed.

Discussion

Combining the relative sea-level curves from the two field areas provides a more complete sea-level history for deposition during the TCC (Figure 19). The sea-level curves show a very close and somewhat surprising match, especially where preserved elevations overlap. The close match is significant for multiple reasons. Firstly, it supports evidence that paleotopography was preserved between the areas. Secondly, it indicates that the two studied areas encountered the same sea-level history and that sea level was at least a regional control (possible global control as stated earlier). The areas preserved a

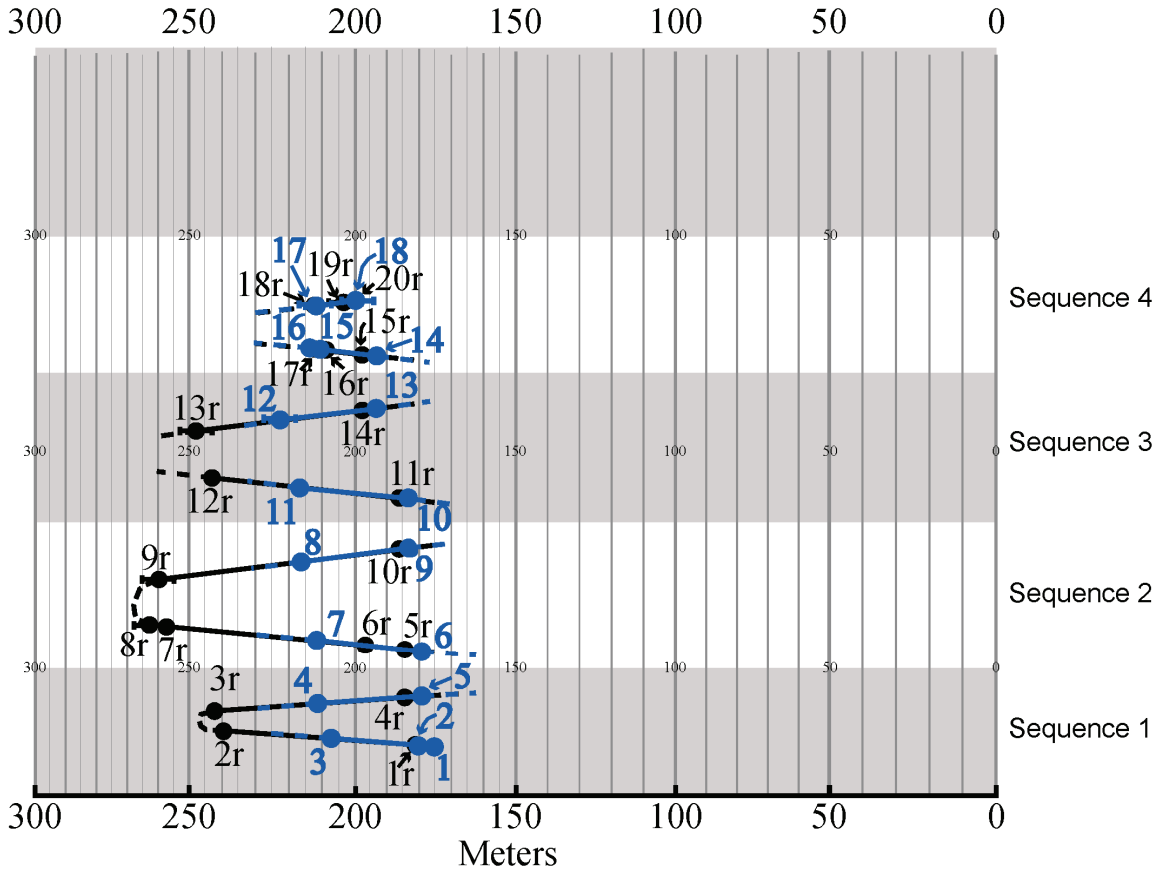

Figure 19: Combined quantitative relative sea-level curve for the La Molata and La Rellana/Ricardillo field areas. The close match of pinning points at overlapping elevations from the two areas indicates paleotopography is preserved and that relative sea level in conjunction with paleotopography was a dominant control on sequence development and character.

similar number of sequences and similar thicknesses, as well as similar lithofacies distribution. Thirdly, the differences between the two areas suggest that local paleogeographic and current controls were significant along with sea level and paleotopography.

Table 2 is a quick overview of the minimum amplitudes of rises and falls for the field areas.

Sequence	Sea-level rise minimum amplitude (m)			Sea-level fall minimum amplitude (m)		
	La Molata	La Rellana/Ricardillo	Total	La Molata	La Rellana/Ricardillo	Total
1	36.5	61.4	67.4	32.3	57.8	63.2
2	37.1	76.6	83.5	33.2	76.2	79.6
3	43.1	60.2	63.6	33.1	49.7	53.6
4	20.6	14.5	20.6	13.7	11.5	13.7

Table 2: Table records the minimum amplitudes of sea-level rises and falls for the studied field areas.

Amplitudes for total sea-level rises and falls range between 53.6-83.5 m. Sequence 4 amplitudes are not used due to it only being preserved as a partial sequence.

Using paleomagnetic data collected from the La Molata field area, Franseen et al. (1998) calculated duration of between 400 ky and 100 ky for TCC deposition that yielded overall accumulation rates of 7.5 to 30.0 cm /ky. The duration of 400 ky to 100 ky for TCC deposition yields an average calculated sequence duration of between 100 ky and 25 ky for the four preserved sequences (Franseen et al. 1998). The relative sea-level curve (Figure 19) shows that relative sea-level rises and falls of 53.6–83.5 m occurred during deposition of the sequences. Using the 400 ky to 100 ky estimate for TCC duration (Franseen et al., 1998) and assuming symmetrical sequences with linear sea-level change, the data indicate rates of relative sea-level rises and falls between 53.6–334 cm/ky. The conservative rates presented here fall within the range measured for Holocene glacio-eustatic rates (Kendall and Schlager, 1981). These calculated rates and amplitudes

documented, along with probable global control discussed earlier and known cyclic glacial activity during the Late Miocene (Mercer and Sutter, 1982), argue for a glacio-eustatic origin.

Results indicate highstand turnaround points for Sequence 1 at approximately 243 m and for Sequence 2 at 263 m. Lowest continuous outcrop of the sequences fall between 175 and 200 m. The sequences are extensive in their lateral distribution, drape (and partially onlap) paleotopography, are relatively thin in thickness as compared to amplitude of sea-level rises and falls, and are relatively uniform in thickness across their distribution.

Paleotopography

The four TCC sequences are considered to be time equivalents across the two studied field areas because of the close match of the relative sea-level curves and similar lithofacies distribution and geometries within the sequences at similar substrate elevations.

Lithofacies	Elevation (m)		Significance
	La Molata	La Rellana/Ricardillo	
Massive ooid grainstone	175-208	181-217	Only in Sequence 3
Thrombolite boundstone	175-180	181-200	Thicker, laterally continuous at low elevations; interbedded with oolites stratigraphically high
Sequence 1 oolites	175-208	181-242.4	Interbeds with more abundant skeletal grains that only occur in Sequence 1
Porites boundstone	175-208	181-246.7	Only in Sequence 3
Digitate stromatolites	175-199	181-197	Only in Sequence 4

Table 3: Table 3 lists the indicative similarities for lithofacies between the field areas. Elevations used in the table are taken from the TCC basement topographic surface.

The similar lithofacies distributions and geometries at similar substrate elevations are suggestive of largely preserved paleotopography. Certain lithofacies only occur in certain sequences and argue for regional depositional changes from sequence to sequence. Differences in lithofacies abundance, distribution and geometries between the areas argue that local controls are significant. The text below, and in the subsequent Build-and-Fill section, discusses the control of paleotopography on the similarities and differences between the field areas.

Local paleotopographic highs and lows in each of the field areas affected lithofacies types, distribution, and geometries in the TCC. The paleovalley at the northeast corner of La Molata persisted through deposition of Sequence 1 and 2, but was subsequently filled by the time of Sequence 3 deposition (Figure 12). The beds within the trough cross-bedded ooid grainstone of Sequence 1 dip and thicken towards the center of the paleotopographic low. Trough cross-bedded ooid grainstone of Sequence 2 thickens in the paleovalley and volcaniclastic-rich planar bedded ooid grainstone fills the paleovalley. The east paleovalley of La Molata persisted through deposition of Sequence 3. Beds within the oolites of Sequence 1, 2, and 3 dip and thicken towards the center of the paleovalley (Figure 13). The northern paleovalley at La Rellana persisted through Sequence 3 deposition, with bedding of Sequence 1 dipping and thickening towards the center of the paleovalley (Figure 14). The southern paleovalley at La Rellana persisted through deposition of Sequences 1 and 2; these sequences lap-out against the southern margin of the paleovalley and Sequence 3 deposits fill in the remaining relief (Figure 16). Where the sequences are deposited over local paleotopographic highs, the beds become thinner and overall thickness of the sequences is decreased (Figure 12). There is a

pronounced steepening at the break in slope of the La Rellana southern margin where paleotopography dips change from 2–5 degrees to more than 11 degrees (Figure 15). At this steeper margin the *Porites* boundstone becomes thicker (up to 6 m) and more laterally continuous (10's of m). The steepening may have concentrated currents at the locations and increased energy allowing for conditions conducive to *Porites* reef production.

Understanding the position of substrate paleotopography relative to sea-level position may allow for prediction of lithofacies distributions and stratal geometries, and is discussed in the subsequent Build-and-Fill section.

Build-and-Fill

Franseen and Goldstein (2004) introduced the concept of build-and-fill sequences. They described a build-and-fill sequence as a laterally extensive sequence that maintained an even thickness, was thin compared to amplitude of sea-level change, tended to drape paleotopography as an entire unit, was capped by a surface of subaerial exposure, and has a complex internal architecture resulting from a topographic building phase and a topographic filling phase. Franseen and Goldstein (2004, 2007) indicated that build-and-fill sequences develop when carbonate production is not optimal, and especially in icehouse systems characterized by high-frequency, high-amplitude sea-level fluctuations. In icehouse ramp/shelf systems, build-and-fill sequences develop in middle or intermediate locations that lie between highstand and lowstand positions, which are areas subjected to the most rapid rates of rises and falls. These settings have a relief-building phase, during sea-level rise, and a relief-filling phase, during sea-level falls.

Franseen and Goldstein (2004, 2007) used the TCC as an example of build-and-fill sequence development, noting that the time of deposition was characterized by extensive glaciation in the southern hemisphere, which created high-frequency high-amplitude sea-level fluctuations, and that the Mediterranean area was a restricted basin; TCC sequences were deposited just after, and perhaps concurrently with evaporite deposition in the main basin and sub-basins. Evaporation may have led to conditions in which carbonate productivity was not optimal.

In this section I use the results of my study to further evaluate the hypothesized build-and-fill model for the TCC, and present a generalized model for TCC sequence development in relation to the well-constrained sea-level curve.

Sequence Thickness, Sea Level Change, and Substrate Elevation

The development of the pinning point curve provides quantitative data on magnitudes of sea-level fluctuations and rates of rise and fall. Minimum amplitudes of sea-level rises and falls ranged between 53.6–83.5 m., whereas the thicknesses of the sequences range from 1.7–12.8 m. The thicknesses of sequences are thin in comparison to the amplitude of sea-level change, meaning that accommodation was left unfilled during deposition. Overall accumulation rates for the sequences were 7.5 to 30.0 cm/ky. Carbonate systems with optimal carbonate productivity have been shown to have accumulation rates that keep up with sea level fluctuations on the order of 200-900 cm/ky (Kendall and Schlager, 1981). Therefore, it appears that carbonate productivity was less than optimal during TCC deposition.

Unlike the other sequences, Sequence 2 in the two areas shows near-complete preservation, without erosion. It captures the highstand turnaround point on La Rellana/Ricardillo (approximately 263 m elevation); La Molata's highest substrate elevations (211.8 m) were too low to provide a shallow water substrate during the highstand turnaround. Neither area preserves sequences at the lowstand turnaround point. On La Molata, Sequence 2 preserves even thickness (3.8-6.7 m) throughout its lateral extent. At the highest elevation of Sequence 2's sea level, the water depth of the shallowest part of La Molata would have been 54 m. Thus, the La Molata substrate was at an intermediate elevation between highstand and lowstand. On La Rellana/Ricardillo this sequence shows abrupt thickening to 5.9 m near the highstand turnaround elevation (between 242 and 257 m). Below those elevations, Sequence 2 is thinner (1.2-3 m), preserves a relatively constant thickness throughout its lateral extent, and drapes 61 m of paleotopography. These observations offer strong support for the build-and-fill model. Where shallow-water substrates exist at the highstand turnaround, sequences thicken. Where substrates lie at intermediate elevations between highstand and lowstand, sequences are thin, drape paleotopography, and maintain constant thickness throughout their lateral extent. This supports the idea of a build-and-fill zone at intermediate elevations between highstand and lowstand.

TCC cyclic sequences appear to be asymmetrical. Oolites are volumetrically the most abundant lithofacies of the TCC and dominate the deposition during the relative falls in sea level. Thrombolite boundstone and *Porites* boundstone deposition are minor components deposited during falls. The relative rises in sea level are dominated by stromatolite and thrombolite boundstone deposition with minor oolite deposition. As will

be discussed below, the TCC sequences at intermediate substrate elevations are characterized by a relief-building phase during relative rises in sea level followed by a relief-filling phase during relative falls in sea level. Limited accommodation due to relative sea-level falls resulted in relatively uniform thicknesses for the sequences across their lateral distribution.

Relative Sea-Level Rise

Sequence 2 at La Molata is used as diagnostic due to its complete sequence preservation across the field area. This sequence is used to build a possible predictive model for sequences that form under the following set of conditions: 1) microbialite-oolite sequences; 2) high-amplitude and high-frequency sea-level fluctuations; 3) with non-optimal carbonate productivity; and 4) at an intermediate elevation relative to sea-level turn-around points (Figure 20). Variations on this model are included from other sequences on La Molata and La Rellana/Ricardillo (below and Appendix XI). These variations can be attributed to paleogeographic controls discussed in the subsequent section.

Sea-level fall after deposition of Sequence 1 left the area exposed subaerially and provided the substrate topography for Sequence 2 deposition (Figure 20A). Sea-level rise over the lowest elevations (179.2-190 m) flooded the area with shallow seas, and deposited stromatolites. The stromatolites are the initial transgressive lithofacies and are deposited in <10 m water depth. Continued sea-level rise flooded the intermediate elevations (190-200 m) of La Molata with shallow seas, and stromatolite deposition continued (Figure 20B). Continued sea-level rise flooded the highest elevations (200-

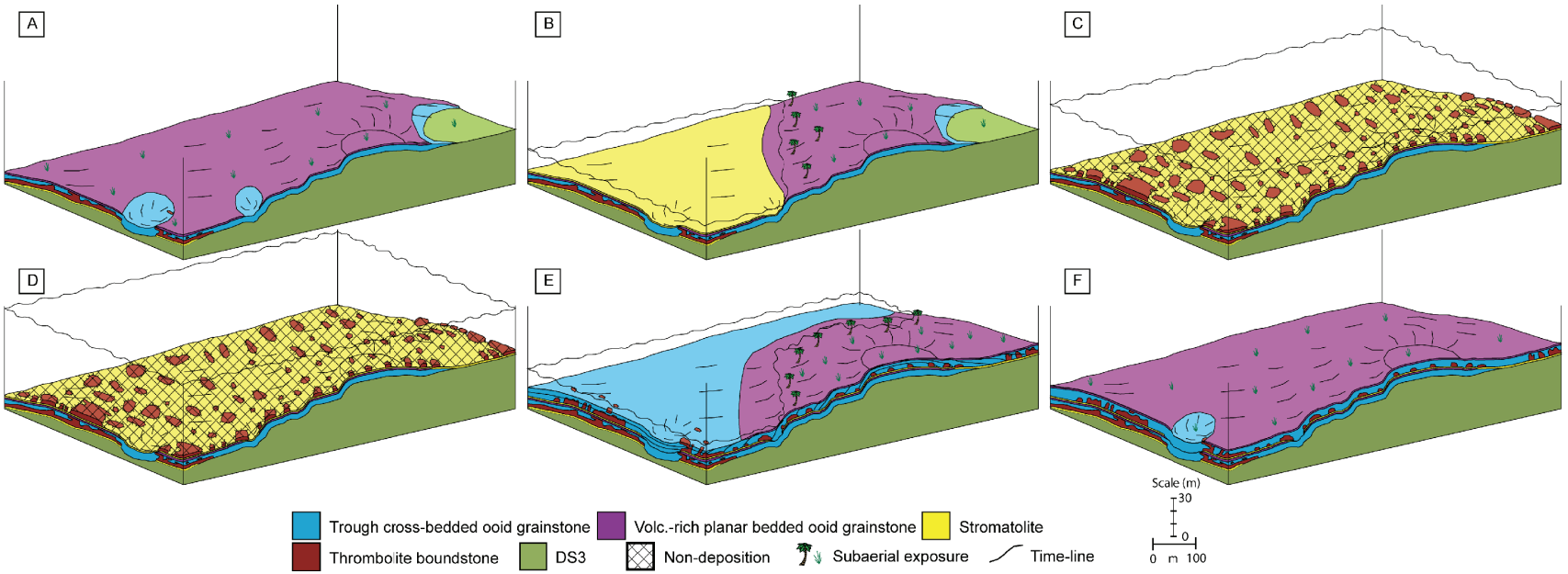

Figure 20: Schematic diagrams of Sequence 2 at La Molata. This well-exposed sequence is helpful in evaluating a build-and-fill model for the microbialite-oolite system. A. Surface for subsequent sequence deposition is subaerially exposed and has local exposure fabrics. B. Stromatolites are thin (0.1-0.7 m) in thickness, drape paleotopography, accumulate in <10 m water depth, and represent the initial transgressive lithofacies. Stromatolite deposition migrates with the sea-level rise and covers the field area. C. Continued sea-level rise freshens the water and thrombolite boundstone deposition began throughout the area representing the later transgressive lithofacies deposited in deeper waters. Thrombolite boundstones are more laterally extensive and thicker at low elevations and are more isolated and thinner at intermediate and high elevations. Ooids likely were generated in nearby shallower waters, but are not preserved in place. D. Continued sea-level rise to the highstand position resulted in 50+ m water depths at the highest elevations on La Molata. With the great water-depths, little, or no, deposition is interpreted during the highstand. E. Sea level began to fall. Continued fall deposited trough cross-bedded ooid grainstone (TCOG) at the highest elevations as the initial regressive lithofacies; it was deposited in <10 m of water depth. Continued sea-level fall migrated TCOG deposition downdip. Volcaniclastic-rich planar bedded ooid grainstone (VPOG) was deposited over the TCOG and was followed by subaerial exposure. The VPOG represents the later regressive lithofacies deposited in <3 m water depth. At the lowest elevations, the TCOB is interbedded with thrombolite boundstones stratigraphically high in the sequence. The thrombolite boundstone deposited during the relative falls accumulate more laterally than vertically. During subaerial exposure, exposure fabrics developed that had fenestral ooid grainstone locally capping sequences. F. Sequence is eventually subaerially exposed with local fenestral ooid grainstone development capping the sequence. During the subaerial exposure, erosion modified the exposed sequence surface, which created the paleotopography for the subsequent sequence deposition.

211.8 m) of La Molata with shallow seas where stromatolites are deposited. After freshening of the water, thrombolite deposition began throughout the area. At the lower elevations, water would have been at least 33 meters deep for deposition of thrombolite boundstone at these elevations. Common ooid grains within the clotted matrix of the thrombolites suggest a nearby source for ooid production existed, perhaps upslope. The thrombolite boundstones at the lowest elevations are laterally extensive (6 to 10s of m wide) and thick (up to 5 m). Accommodation space created from sea-level rise allowed for the thrombolite boundstones to build vertically and form constructional relief. Continued sea-level rise would have the highest elevations of La Molata under about 54 m of water by comparison to the highstand elevation on La Rellana/Ricardillo. As sea level rose toward those elevations, thrombolite boundstone deposition at La Molata may have continued with thrombolite deposition building relief (Figure 20C). Thrombolite boundstone at the intermediate and high elevations are more isolated (<3 m wide) and thinner (<2 m) possibly reflecting more limited accommodation space to grow vertically. As sea level rose to its highest position, it is hypothesized that water was so deep, that there was little or no deposition on La Molata (Figure 20D), but this hypothesis cannot be confirmed. At the same time at the high elevations (220-262.7) of La Rellana/Ricardillo, accumulating lithofacies were isolated thrombolite boundstone interbedded with trough cross-bedded ooid bivalve grainstone. The trough cross-bedded ooid bivalve grainstone is interpreted to be deposited in <10 m water depth indicating that the thrombolite boundstones deposited at the high elevations of La Rellana/Ricardillo were deposited in <10 m water depth.

The contact between the stromatolites and overlying thrombolite boundstone can be gradational, and in rare instances within Sequence 4, the lithofacies are interbedded stratigraphically low in the sequence. Minor oolites are interpreted to have been deposited during the relative rises in sea level. Sequence 2 has trough cross-bedded ooid bivalve grainstone interbedded with thrombolite boundstone forming the basal lithofacies at high elevations of La Rellana/Ricardillo (Figure 15). The low elevations for Sequence 2 at La Rellana/Ricardillo have rare trough cross-bedded ooid bivalve grainstone forming the basal lithofacies. Sequence 2 at La Molata has one location with the trough cross-bedded ooid bivalve grainstone lithofacies forming the base of the sequence, which would have eroded the stromatolite lithofacies (Figure 12). Where the trough cross-bedded ooid bivalve grainstone occurs as the basal lithofacies at these locations, thrombolite boundstone overlies it. On the eastern margin of the central high at La Molata, Sequence 3 has stromatolite overlain by trough cross-bedded ooid grainstone overlain by massive ooid grainstone that grades upward to trough cross-bedded ooid grainstone (Figure 12). The trough cross-bedded ooid grainstone above the stromatolite may have been deposited during the relative rise in sea level. Overall, however, the relative rises in sea level are dominated by microbialites that build topographic relief.

Relative Sea-Level Fall

From the sea level highstand in Sequence 2 (263 m) sea-level fell at least 41 m, renewing shallow-water deposition on the highest substrates on La Molata and depositing trough cross-bedded ooid grainstone as the initial regressive lithofacies. The trough cross-bedded ooid grainstone fills in the topographic relief of the thrombolite boundstones and

beds lap out against them. The contact between thrombolite boundstone and trough cross-bedded ooid grainstone is a sharp, and in places, erosive contact. As sea level continued to fall, trough cross-bedded ooid grainstone deposition migrated downdip, and updip deposits were overlain by shallower water volcaniclastic-rich planar bedded ooid grainstone and then fenestral fabrics, indicating subaerial exposure. Continued sea-level fall to intermediate elevations led to downdip deposition of volcaniclastic-rich planar bedded ooid grainstone and subsequent subaerial exposure. At lower elevations, trough cross-bedded ooid grainstone is deposited along with thrombolite boundstone (Figure 20E). The thrombolite boundstones deposited during the relative falls in sea level accumulate laterally (1 m up to 10's of m) with little vertical component (commonly 1 m thick) due to limited accommodation (Figure 13). The trough cross-bedded ooid grainstone thickens in paleotopographic lows and thins over paleotopographic highs due to limited accommodation (Figure 14). Continued sea-level fall resulted in deposition of volcaniclastic-rich planar bedded ooid grainstone, fenestral ooid grainstone, and subaerial exposure (Figure 20F).

The relative sea-level falls are dominated by oolite deposition with trough cross-bedded ooid grainstone commonly as the initial regressive deposits. Sequence 3, however, has massive ooid grainstone as the initial regressive lithofacies and Sequence 1 at La Rellana/Ricardillo has bioturbate ooid grainstone as the initial regressive lithofacies. The oolites drape paleotopography and fill limited accommodation during the relative falls in sea level. Also, minor thrombolite boundstone and *Porites* boundstone were deposited during the relative sea-level falls. At the lowest elevations in Sequences 1 and 2 at La Molata and Sequence 2 at La Rellana/Ricardillo, thrombolite boundstone is

interbedded with trough cross-bedded ooid grainstone stratigraphically high in the sequences. Sequence 3 at La Molata has thrombolite boundstone interbedded with massive ooid grainstone stratigraphically low in the sequence and interbedded with trough cross-bedded ooid grainstone above massive ooid grainstone. Sequence 3 at both locations has *Porites* boundstone interbedded with trough cross-bedded ooid grainstone. These thrombolite boundstones and *Porites* boundstones built minor topographic relief during the relative sea-level falls. Overall, however, the relative falls in sea level are predominated by oolites filling in topographic relief.

Climate, Paleogeography, and Currents

Biota through Time

Lithofacies and biotic constituents in the sequences from both areas indicate that regional marine conditions changed from more restricted to more normal from Sequence 1 through Sequence 3 (Sequence 4 is excluded due to only partial preservations). This change from more restricted to more normal marine conditions is evidenced by the following characteristics from the areas. Calcareous red-algae are much more abundant in the thrombolite boundstone of Sequence 2 at La Molata (up to 70% with averages between 20 – 50%) than thrombolite boundstone of Sequence 1 (0-10%) indicating more normal marine conditions during deposition of Sequence 2. Overall, the oolites of Sequence 2 have much more abundant skeletal grains (commonly 10-20%) than the oolites of Sequence 1 (commonly 5-15%) at La Rellana/Ricardillo. The *Porites* boundstone lithofacies is found only in Sequence 3 at both field locations and consists of a diverse biota assemblage indicating the most normal marine conditions during TCC deposition.

One hypothesis to explain this biotic development can be by increasing circulation of open ocean waters successively with each sequence. This could be induced tectonically by progressively opening deeper straits into the Mediterranean (Rouchy and Saint Martin, 1992; Esteban, 1996), but this hypothesis remains untested. Alternatively, increasing biotic diversity can be explained by having each successive sea level highstand be higher than the previous one. The highstand position for Sequence 2 is indeed higher than for Sequence 1, and the highstand elevation of Sequence 3 is unknown. On the other hand, if biotic diversity were related to elevation of sea level, then one would expect decreasing diversity and evidence for increased restriction during regressive parts of sequences. The biotic diversity, on the contrary is preserved late in the regressive parts of the sequences, thus arguing against this control.

Another hypothesis to explain increasing diversity is climate control with decreasing aridity through time. It is well known that the TCC forms immediately after deposition of evaporites in the Mediterranean (Esteban, 1979; Esteban and Giner, 1980, Dabrio et al., 1981; Rouchy and Saint Martin, 1992; Martin and Braga, 1994). It is also well known that the latest Messinian phase in the Mediterranean is dominated by the Lago Mare fresh-to-brackish deposits. This long-term decrease in aridity could easily be reflected in increasing biotic diversity in the TCC.

Paleogeographic Controls

There are four major biotic, lithofacies, and architectural differences between the two field areas, indicating that local paleogeography and currents were important in controlling sequence character.

(1) The stromatolite boundstone lithofacies varies in distribution, preservation, and morphology within sequences and between field areas. In Sequence 1 of La Molata (Figure 12), the lowest elevations (175-180 m) have laterally continuous stromatolites, but at La Rellana/Ricardillo (Figure 15) there are no stromatolites at the lowest elevation (181 m). Sequence 2 at La Molata has laterally continuous stromatolites at the low elevations with local stromatolites at intermediate to high elevations. La Rellana/Ricardillo has no stromatolites throughout Sequence 2.

(2) Sequence 3 shows significant differences in lithofacies between the two areas, which appears to highlight current circulation differences between the two areas. Thrombolite boundstone is more abundant in Sequence 3 on La Molata as compared to La Rellana. *Porites* boundstone only occurs in Sequence 3 in both areas, but its abundance and nature of occurrence is significantly different between the areas. At La Molata, only four isolated (up to 1.7 m wide and 2 m thick) *Porites* boundstone patch reefs occur. In contrast, *Porites* boundstone is more abundant at La Rellana/Ricardillo where the *Porites* boundstone is laterally continuous and thick (up to 10's of m wide and 6.2 m thick) at the lowest elevations and small (commonly <3 m wide and 2 m thick), isolated patch reefs at intermediate to high elevations.

(3) At the lowest elevations, Sequence 1 at La Molata has laterally continuous thrombolite boundstone that is interbedded with trough cross-bedded ooid grainstone stratigraphically higher in the section, whereas La Rellana/Ricardillo has no thrombolite boundstone. Only beach lithofacies were deposited at the lowest elevations of La Rellana/Ricardillo.

(4) The greater abundance of skeletal grains in several sequences in the La Rellana/Ricardillo area, compared to La Molata, is suggestive of more normal marine conditions in the La Rellana/Ricardillo area. Skeletal grains in the form of bivalves and gastropods are rare (0-5%) within the trough cross-bedded ooid grainstone of Sequence 2 at La Molata. At La Rellana/Ricardillo, the skeletal grains are common to abundant (3-37%) within the trough cross-bedded ooid grainstone of Sequence 2. Skeletal grains are rare (0-8%) within the trough cross-bedded ooid grainstone of Sequence 3 at La Molata. At La Rellana/Ricardillo, skeletal grains in the form of bivalves, gastropods, and serpulid worms are common to abundant (2-44%).

Overall, it appears that local paleogeographic differences between the two areas led to more restricted conditions for the La Molata area and more open marine conditions for the La Rellana/Ricardillo area. Presence of more stromatolites at La Molata may indicate more restriction, whereas beach lithofacies at La Rellana/Ricardillo indicate an open connection. The more abundant, thicker, and more laterally continuous *Porites* boundstone deposits at La Rellana/Ricardillo, as opposed to thrombolites at La Molata, argue that conditions were more conducive to coral development at La Rellana/Ricardillo. This is likely caused by more normal marine conditions with better wave energy at the La Rellana/Ricardillo field areas as opposed to the relatively more restricted waters at La Molata.

The paleogeography that led to open marine conditions and high wave energy at La Rellana/Ricardillo, and more restriction at La Molata, can be inferred from the regional geology, and by inferring a dominant swell direction similar to that of the modern system coming from the east and northeast. La Rellana/Ricardillo carbonates are

essentially facing east and paleohighs existed to the west and northwest. An embayment caused by topography from the Rodalquilar caldera protruded west into the coast line just south of this area. La Molata was located within the northern margin of this reentrant, most likely sheltered from much of the east-southeast-directed currents (Figure 3).

CONCLUSIONS

1) Upper Miocene microbial (thrombolite, stromatolite), oolitic, coral reef, and bioclastic carbonate sequences in two southeast Spain study locations were deposited in association with high-amplitude glacioeustacy and evaporitic drawdown. Both study areas preserve paleotopography; La Molata has 33 m of paleotopographic relief over 0.86 km and La Rellana/Ricardillo has 76 m of paleotopographic relief over 1.63 km. Taken together, the two areas have a total of 82 m of paleotopographic relief preserved.

2) Each area preserves four cyclic sequences that are laterally extensive, and some maintain uniform thicknesses. The four sequences at the La Molata and La Rellana/Ricardillo field areas are considered to be time-equivalents. The close match of the quantitative relative sea-level curves and similar lithofacies distribution is suggestive of largely preserved paleotopography.

3) For low elevations a sequence has basal stromatolite overlain by local laterally continuous thrombolite boundstone that becomes interbedded with and eventually overlain by trough cross-bedded ooid grainstone. The trough cross-bedded ooid grainstone grades upward to volcaniclastic-rich planar bedded ooid grainstone capped by fenestral ooid grainstone.

4) For high elevations a sequence has local stromatolite, overlain by local isolated thrombolite boundstone, overlain by trough cross-bedded ooid grainstone. The trough cross-bedded ooid grainstone grades upward to volcaniclastic-rich planar bedded ooid grainstone capped by fenestral ooid grainstone.

5) Quantitative relative sea-level curves created for both areas show a close match and indicate similar sea-level histories. Amplitudes of total sea-level rise and fall ranged from 53.6-83.5 m and were induced by glacio-eustacy. During the sea-level rises, microbialites draped and built topographic relief. During the sea-level falls, oolites filled in topographic relief. Minor thrombolite boundstones deposited during the sea-level fall accumulated more laterally than vertically due to limited accommodation. Some *Porites* reefs also formed during a relative sea-level fall, and built minor relief.

6) Where the substrates were in shallow water at highstand, the sequence thickens. Downslope, in areas where substrate elevation was intermediate between highstand and lowstand, sequences are thinner and of even thickness. This supports the idea that much of the substrate is within the intermediate elevation build-and-fill zone proposed by Franseen and Goldstein.

7) The sequences are depositionally asymmetrical, with the majority of the deposition occurring during the relative fall in sea-level. A build-and-fill model is proposed for oolite-microbialite systems forming during high-amplitude high-frequency sea-level fluctuations at intermediate substrate elevations relative to sea-level turn-around points. Possibly predictive lithofacies distributions and geometries from the model include:

a) Stromatolites are the initial transgressive lithofacies of the sequences. They are more laterally continuous at the low elevations where they are commonly overlain by thrombolite boundstone.

b) Thrombolite boundstones are the later transgressive deposits and are thicker and more laterally continuous at the low elevations.

c) At intermediate to high elevations, thrombolite boundstones become more isolated.

d) Trough cross-bedded ooid grainstones are commonly the initial regressive lithofacies that fill in topographic lows and drape (partially onlap) paleotopography.

e) At low elevations, regressive thrombolite boundstones are interbedded with trough cross-bedded ooid grainstone and accumulate more laterally than vertically.

f) Volcaniclastic-rich planar bedded ooid grainstones are the latest regressive deposits that preserve the last depositional lithofacies of the sequences.

g) Sequences are commonly capped by fenestral ooid grainstones representing subaerial exposure.

8) Increasing biotic diversity through time is best explained by decreasing aridity during the latest parts of the Messinian.

9) Areas within an embayment were protected from waves and more restricted than areas open to the east and northeast. Open areas preserve more coral reefs and oolite whereas restricted areas favor thrombolites and stromatolites.

10) Results from this study can aid in predicting lithofacies distribution and geometries in outcrop and the subsurface for cyclic oolite-microbialite-coralgal reef systems.

11) Comprehension of the depositional controls of paleotopography, relative sea level, and paleogeography are essential to understanding and predicting lithofacies distributions and geometries for the TCC.

REFERNCES CITED

ADAMS, E.W., SCHRODER, S., GROTZINGER, J.P., AND MCCORMICK, D.S., 2004, Digital Reconstruction and Stratigraphic Evolution of a Microbial-Dominated, Isolated Carbonated Platform (Terminal Proterozoic, Nama Group, Namibia): Journal of Sedimentary research, v. 74, p. 479-497.

ADAMS, E.W., GROTZINGER, J.P., WATTERS, W.A., SCHRODER, S., MCCORMICK, D.S., AND AL-SIYABI, H.A., 2005, Digital characterization of thrombolite-stromatolite reef distribution in a carbonate ramp system [terminal Proterozoic, Nama Group, Namibia]: AAPG Bulletin, v. 89, p. 1293-1318.

AL-SAAD, H., AND SADOONI, F.N., 2001, A new depositional model and sequence stratigraphic interpretation for the Upper Jurassic Arab "D" reservoir in Qatar: Journal of Petroleum Geology, v. 24, p. 243-264.

AL-SUWAIDI, A.S., TAHER, A.K., ALSHARHAN, A.S. AND SALAH, M.G., 2000, Stratigraphy and geochemistry of Upper Jurassic Diyab Formation, Abu Dhabi, U.A.E.: Special Publication – Society for Sedimentary Geology, v. 69, p. 249-271.

ARRIBAS JR., A., CUNNINGHAM, C.G., RYTUBA, J.J., RYE, R.O., KELLY, W.C., PODWYSOCKI, M.H., MCKEE, E.H., AND TOSDAL, R.M., 1995, Geology, Geochronology, Fluid Inclusions, and Isotope Geochemistry of the Rodalquilar Gold Alunite Deposit, Spain: Economic Geology, v. 90, p. 795-822.

AURELL, M., AND BADENAS, B., 1997, The pinnacle reefs of Jabaloyas (Late Kinmmeridgian, NE Spain): Vertical zonation and associated facies related to sea level changes: Cuadernos de Geologia Iberia, v. 22, p. 37-64.

BALL, M.M., 1967, Carbonate Sand Bodies of Florida and the Bahamas: Journal of Sedimentary Petrology, v. 37, p. 556-571.

BATTEN, K.L., NARBONNE, G.M., AND JAMES, N.P., 2004, Paleoenvironments and growth of early Neoproterozoic calcimicrobial reefs: platformal Little Dal Group, northwestern Canada: Precambrian Research, v.133, p. 249-269.

BISHOP, M.G., 2000, Petroleum Systems of the Northwest Java Province, Java and Southeast Offshore Sumatra, Indonesia: Open-file Report 99-50R.

BOGGS JR., S., 1995, principles of sedimentology and stratigraphy: Prestice Hall, 2nd edition, 774 p.

BRACHERT, T.C., BETZLER, C., BRAGA, J.C., AND MARTIN, J.M., 1998, Microtaphofacies of a Warm-Temperate Carbonate Ramp (Uppermost Tortonian/Lowermost Messinian, Southern Spain): Palaios, v. 13, p. 459-475.

BRACHERT, T.C., HULTZSCH, N., KNOERICH, A.C., KRAUTWORST, U., AND STUCKRAD, O.M., 2001, Climatic signatures in shallow-water carbonates: high-resolution stratigraphic markers in structurally controlled carbonate buildups (Late Miocene, southern Spain): Palaeogeography, Palaeoclimatology, Palaeoecology, v. 175, p. 211-237.

BRAGA, J.C., AND MARTIN, J.M., 1988, Neogene coralline-algal growth-forms and their paleoenvironments in the Almanzora river valley (Almeria, S.E. Spain): Paleogeography, Paleoclimate, and Paleoecology, v. 67, p. 285-303.

BRAGA, J.C., AND MARTIN, J.M., 1992, Messinian carbonates of the Sorbas Basin: sequence stratigraphy, cyclicity, and facies, *in* Franseen, E.K., Esteban, M., Ward, W.C., and Rouchy, J.-M., eds., Models for Carbonate Stratigraphy from Miocene Reef Complexes of the Mediterranean Regions, SEPM Concepts in Sedimentology and Paleontology Series No. 5, p. 78-108.

BRAGA, J.C., MARTIN, J.M., AND RIDING, R., 1995, Controls on Microbial Dome Fabric Development along a Carbonate-Siliciclastic Shelf-Basin Transect, Miocene, SE Spain: PALAIOS, v. 10, p. 347-361.

BUCHHEIM, P.H., 2009, Pale environmental Factors Controlling Microbialite Bioherm Deposition and Distribution in the Green River Formation: Geological Society of America Abstracts with Programs, v. 41, p. 511.

BURCHETTE, T.P., AND WRIGHT, V.P., 1992, Carbonate ramp depositional systems: Sedimentary Geology, v. 79, p. 87-115.

CALVET, F., ZAMARRENO, I., AND VALLES, D., 1996, Late Miocene Reefs of the Alicante-Elche Basin, Southeast Spain, *in* Franseen, E.K., Esteban, M., Ward, W.C., and Rouchy, J.-M., eds., Models for Carbonate Stratigraphy from Miocene Reef Complexes of the Mediterranean Regions, SEPM Concepts in Sedimentology and Paleontology Series No. 5, p. 177-190.

CALVO, M., OSETE, M.L., AND VEGAS, R., 1994, Paleomagnetic rotations in opposite senses in southeastern Spain: Geophysical Research Letters, v. 21, p. 761-764.
CORNEE, J.J., SAINT MARTIN, J.P., CONESA, G., AND MULLER J., 1994, Geometry, palaeoenvironments and relative sea-level (accommodation space) changes in the Messinian Murdjado carbonate platform (Oran, western Algeria): consequences: Sedimentary Geology, v. 89, p., 143-158.
CUNNINGHAM, C.G., ARRIBAS JR., A., RYTUBA, J.J., AND ARRIBAS, A., 1990, Mineralized and unmineralized calderas in Spain; Part I, evolution of the Los Frailes Caldera: Mineralium Deposita, v25 (suppl.), p. S21-S28.
CUNNINGHAM, K.J., 1995, An upper Miocene sedimentary succession, Melilla basin, northeastern Morocco [unpublished Unpublished PhD thesis]: University of Kansas, Lawrence, KS, 371 p.
DABRIO, C.J., ESTEBAN, M., AND MARTIN, J.M., 1981, The Coral Reef of Nijar, Messinian (Uppermost Miocene), Almeria Province, SE Spain: Journal of Sedimentary Petrology, v. 51, p. 521-439.
DAVIES, R., HOOLIS, C., BISHOP, C., GUAR, R., AND HAIDER, A.A., 2000, Reservoir Geology of the Middle Minagish Member (Minagish Oolite), Umm Gudair Field, Kuwait: Special Publication Society for Sedimentary Geology, v. 69, p. 273-286.
DILLETT, P.M., 2004, Paleotopographic and sea-level controls on the sequence stratigraphic character of a heterozoan carbonate succession: Pliocene, Carboneras basin, southeast Spain [unpublished Unpublished M.S. thesis]: University of Kansas, Lawrence, KS, 116 p.
DRONKERT, H., 1976, Late Miocene Evaporites in the Sorbas Basin and Adjoining Areas: Memorie della Societa Geologica Italiana, v. 16, p. 341-361.
DVORETSKY, R.A. 2009, Stratigraphy and reservoir-analog modeling of upper Miocene shallow-water and deep-water carbonate deposits: Agua Amarga basin, southeast Spain [unpublished Unpublished M.S. thesis]: University of Kansas, Lawrence, KS, 138 p.
ESTEBAN, M., 1979, Significance of the Upper Miocene Coral Reefs of the Western Mediterranean: Palaeogeography, palaeoclimatology, palaeoecology, v 29, p. 169-188.
ESTEBAN, M., 1996, An Overview of Miocene Reefs from Mediterranean Areas: General Trends and Facies Models, *in* Franseen, E.K., Esteban, M., Ward, W.C., and Rouchy, J.-M., eds., Models for Carbonate Stratigraphy from Miocene Reef Complexes of the Mediterranean Regions, SEPM Concepts in Sedimentology and Paleontology Series No. 5, p. 3-54.
ESTEBAN, M., AND GINER, J., 1980, Messinian coral reefs and erosion surfaces in Cabo de Gata (Almeria, SE Spain): Acta Geologica Hispanica, v. 15, p. 97-104.
ESTEBAN, M., AND KLAPPA, C.F., 1983, Subaerial exposure environments, *in* Scholle, P.A., Bebout, D.G., and Moore, C.H., eds., Carbonate depositional environments: AAPG Memoir 33, p. 2-54.
ESTEBAN, M., BRAGA, J.C., MARTIN, J., AND SANTISTEBAN, C., 1996, Western Mediterranean Reef Complexes, *in* Franseen, E.K., Esteban, M., Ward, W.C., and Rouchy, J.-M., eds., Models for Carbonates Stratigraphy from Miocene Reef Complexes of Mediterranean Regions, SEPM Concept in Sedimentology and Paleontology, p. 55-72.
ESTEBAN, M., CALVET, F., DABRIO, C., BARON, A., GINER, J., POMAR, L., SALAS, R., AND PERMANYER, A., 1978, Aberrant features of the Messinian coral reefs, Spain: Acta Geologica, v. 13, p. 20-22.
FELDMANN, M., AND MCKENZIE, J.A., 1997, Messinian stromatolite-thrombolite associations, Santa Pola, SE Spain: an analogue for the Palaeozoic?: Sedimentology, v. 44, p. 893-914.
FELDMANN, M., AND MCKENZIE, J.A., 1998, Stromatolite-Thrombolite Associations in a Modern Environment, Lee Stocking Island, Bahamas: PALAIOS, v. 13, p. 201-212.
FERNANDEZ-SOLER, J.M., 1996, Volcanics of the Almeria Province, *in* Mather, A.E., Martin, J.M., Harvey, A.M., and Braga, J.C., eds., A Field Guide to the Geology and Geomorphology of the Neogene Sedimentary Basins of the Almeria Province, SE Spain: Oxford, Blackwell, p. 58-88.
FLUGEL, E., 1982, Microfacies Analysis of Limestones: New York, Springer-Verlag, p. 106-129.
FORNOS, J.J., AND Ahr, W.M., 1997, Temperate carbonates on a modern, low-energy, isolated ramp; the Belearic Platform, Spain: Journal of Sedimentary Research, v. 67, p. 364-373.
FRANSEEN, E.K., AND GOLDSTEIN, R.H., 1996, Paleoslope, Sea-level and Climate Controls on Upper Miocene Platform Evolution, Las Negras Area, Southeastern Spain, *in* Franseen, E.K., Esteban, M., Ward, W. C., and Rouchy, J.-M., eds., Models for Carbonates Stratigraphy from Miocene Reef Complexes of Mediterranean Regions, SEPM Concept in Sedimentology and Paleontology, p. 159-176.

FRANSEEN, E.K., AND GOLDSTEIN, R.H., 2004, Build-and-Fill: A Stratigraphic Pattern Induced in Cyclic Sequences by Sea Level and Paleotopography: Geological Society of America Abstracts with Programs, v. 36, p. 377.

FRANSEEN, E.K., AND MANKIEWICZ, C., 1991, Depositional sequences and correlation of middle(?) to late Miocene carbonate complexes, Las Negras and Nijar areas, southeastern Spain: Sedimentology, v. 38, p. 871-898.

FRANSEEN, E.K., GOLDSTEIN, R.H., AND ESTEBAN, M., 1997a, Controls on Porosity Types and Distribution in Carbonate Reservoirs: A Guidebook for Miocene Carbonate Complexes of the Cabo de Gata Area, SE Spain: American Association of Petroleum Geologists Education Program, p. 1-150.

FRANSEEN, E.K., GOLDSTEIN, R.H., AND FARR, M.R., 1997b, Substrate-Slope and Temperature Controls on Carbonate Ramps: Revelations from Upper Miocene Outcrops, SE Spain, *in* James, N.P., and Clarke, A.D., eds., Cool-Water Carbonates, SEPM Special Publication, p. 271-290.

FRANSEEN, E.K., GOLDSTEIN, R.H., AND FARR, M.R., 1998, Quantitative Controls on Location and Architecture of Carbonate Depositional Sequences: Upper Miocene, Cabo de Gata Region, SE Spain: Journal of Sedimentary Research, v. 68, p. 283-298.

FRANSEEN, E.K., GOLDSTEIN, R.H., AND WHITESELL, T.E., 1993, Sequence stratigraphy of Miocene carbonate complexes, Las Negras area, southeastern Spain: implications for quantification of changes in relative sea-level, *in* Loucks, R.G., and Sarg, J.F., eds., Carbonate Sequence Stratigraphy: Recent Developments and Applications, AAPG Memoir 57, p. 409-434.

GIBBONS, W., AND MORENO, M.T., eds., 2003, The Geology of Spain: Geological Society of London, p. 649.

GOLDSTEIN, R.H., AND FRANSEEN, E.K., 1995, Pinning points: a method providing quantitative constraints on relative sea-level history: Sedimentary Geology, v. 95, p. 1-10.

GROTZINGER, J.P., AND KNOLL, A.H., 1999, Stromatolites in Precambrian Carbonates: Evolutionary Mileposts or Environmental Dipsticks?: Annual Review of Earth and Planetary Sciences, v. 27, p. 313-358.

GROTZINGER, J.P., WATTERS, W.A., AND KNOLL, A.H., 2000, Calcified metazoans in thrombolite-stromatolite reefs of the terminal Proterozoic Nama Group, Namibia: Paleobiology, v. 26, p. 334-359.

HARRIS, P.H., 1977, The Joulters ooid shoal, Great Bahama Bank, *in* Peryt, T.M., ed., Coated grains: New York, Springer-Verlag, p. 132-141.

HINE, A.C., 1977, Lily Bank, Bahamas; history of an active oolite shoal: Journal of Sedimentary Petrology, v. 47, p. 1554-1581.

HOFFMAN, P., 1967, Algal Stromatolites: Use in Stratigraphic Correlation and Paleocurrent Determination: Science, v. 157, p. 1043-1045.

HOLAIL, H.M., KOLKAS, M.M., AND FRIEDMAN, G.M., 2006, Facies analysis and petrophysical properties of the lithologies of the North Gas Field, Qatar: Carbonates and Evaporites, v. 21, p.40-50.

HONDA, N., OBATA, Y., AND ABOUELENEIN, M.K.M., 1989, Petrology and Diagenetic Effects of Carbonate Rocks: Jurassic Arab C Oil Reservoir in El Bundug Field, Offshore Abu Dhabi and Qatar: SPE 6th Middle East Oil Show, p. 787-796.

HSU, K.J., RYAN, W.B., AND CITA, M.B., 1973, Late Miocene Desiccation of the Mediterranean: Nature, v. 242, p. 240-244.

HSU, K.J., MONTADERT, L., BEROULLI, D., CITA, M.B., ERICKSON, A., GARRISON, R.E., KIDD, R.B., MELIERES, F., MULLER, C., AND WRIGHT, R., 1977, History of the Mediterranean salinity crisis: Nature, v. 267, p. 399-403.

HANFORD, C.R., AND LOUCKS, R.G., 1993, Carbonate depositional sequences and systems tracts; responses of carbonate platforms to relative sea-level changes, *in* Loucks, R.G., and Sarg, J.F., eds., Carbonate sequence stratigraphy; recent developments and application: AAPG Memoir 57, p. 3-41.

HEYDARI, E., AND BARIA, L., 2005, A Microbial Smackover Formation and the Dual Reservoir-Seal System at the Little Cedar Creek Field in Conecuh County of Alabama: Gulf Coast Association of Geological Societies Transactions, v. 55, p. 294-320.

HITZMAN, D., 1996, Microbial reservoir characterization; and integration of surface geochemistry and development geology data: Annual Meeting Expanded Abstracts – American Association of Petroleum Geologists, v. 5, p. 65.

INDEN, R.F., AND MOORE, C.H., 1983, Beach Environment, *in* Scholle, P.A., Bebout, D.G., and Moore, C.H., eds., Carbonate Depositional Systems: AAPG Memoir 33, p. 212-265.
JOHNSON, C.L., FRANSEEN, E.K., AND GOLDSTEIN, R.H., 2005, The effects of sea level and paleotopography on lithofacies distribution and geometries in heterozoan carbonates, south-eastern Spain: Sedimentology, v. 52, p. 513-536.
KENDALL, C.G.ST.C., AND SCHLAGER, W., 1981, Carbonates and relative changes in sea level: Marine Geology, v. 44, p. 181-212.
LIONELLO, P., AND SANNA, A., 2005, Mediterranean wave climate variability and its links with NAO and Indian Monsoon: Climate Dynamics, v. 25, p. 611-623.
LLINAS, J.C., 2002, Diagenetic history of the Upper Jurassic Smackover Formation and its effects on reservoir properties; Vocation Field, Manila Sub Basin, eastern Gulf Coastal Plain.: Gulf Coast Association of Geological Societies and Gulf Coast Section SEPM, technical papers and abstracts, v. 52, p. 631-644.
LLINAS, J.C., 2003, Petroleum Exploration for Upper Jurassic Smackover Carbonate Shoal and Microbial Reefal Lithofacies Associated with Paleohighs, Southwest Alabama: Gulf Coast Association of Geological Societies, v. 53, p. 462-474.
LLOYD, R.M., PERKINS, R.D., AND KERR, S.D., 1987, Beach and shoreface ooid deposition on shallow interior banks, Turks and Caicos Islands, British West Indies: Journal of Sedimentary Petrology, v. 57, p. 976-982.
LOPEZ-RUIZ, J., AND RODRIGUEZ-BADIOLA, E., 1980, La Region Volcanica Neogena del Sureste de Espana: Estudios Geologicos, v. 36, p. 5-63.
LOREAU, J.P., AND PURSER, B.H., 1973, Distribution and ultrastructure of Holocene ooids in the Persian Gulf, *in* Purser, B.H., eds., The Persian Gulf, Holocene Carbonate Sedimentation in a Shallow Epicontinental Sea: New York, Springer-Verlag, p. 279-328.
LU, G., AHARON, P., AND MCCABE, C.W., 1996, Magnetostratigraphy of the uplifted former atoll of Niue, South Pacific: implications for accretion history and carbonate diagenesis: Sedimentary Geology, v. 105, p. 259-274.
MAJOR, R.P., BEBOUT, D.G., AND HARRIS, P.M., 1996, Recent evolution of a Bahamian ooid shoal; effects of Hurricane Andrew: GSA Bulletin, v. 108, p. 168-180.
MANCINI, E.A., AND PARCELL, W.C., 2001, Outcrop Analogs for Reservoir Characterization and Modeling of Smackover Microbial Reefs in the Northeastern Gulf of Mexico Area: Gulf Coast Association of Geological Societies Transactions, v. 51, p. 207-218.
MANCINI, E.A., PARCELL, W.C., BENSON, J.D., CHEN, H., AND YANG, W.,-T., 1998, Geological and Computer Modeling of Upper Jurassic Smackover Reef and Carbonate Shoal Lithofacies, Eastern Gulf Coastal Plain: Gulf Coast Association of Geological Societies Transactions, v. 48, p. 225-234.
MANCINI, E.A., PARCELL, W.C., AHR, W.M., RAMIREZ, V.O., LLINAS, J.C., AND CAMERON, M., 2008, Upper Jurassic updip stratigraphic trap and associated Smackover microbial and nearshore carbonate facies, eastern Gulf coastal plain: AAPG Bulletin, v. 92, p. 417-442.
MANCINI, E.A., LLINAS, J.C., PARCELL, W.C., AURELL, M., BADENAS, B., LEINFELDER, R.R., AND BENSON, J.D., 2004, Upper Jurassic thrombolite reservoir play, northeastern Gulf of Mexico: AAPG Bulletin, v. 88, p. 1573-1602.
MANKIEWICZ, C., 1996, The Middle to Upper Miocene carbonate complex of Nijar, Almeria Province, southeastern Spain, *in* Franseen, E.K., Esteban, M., Ward, W.C., and Rouchy, J.-M., eds., Models for Carbonates Stratigraphy from Miocene Reef Complexes of Mediterranean Regions, SEPM Concept in Sedimentology and Paleontology.
Mapa Excursionis Y Turistico: Cabo de Gata Nijar Parque Natural: Editorial Alpina. 2001.
Mapa Topografico Nacional de Espana: Las Negras: Ministerio de Fomento, Instituto Geografico Nacional. 1998
MARCAL, R.A., SPADINI, R.A., AND RODRIGUEZ, R.A., 1998, Influence of sedimentation and early diagenesis on the permoporosity of carbonate reservoirs of Macae Formation, Campos Basin, Brazil: AAPG Bulletin, v. 82, p. 1938.
MARTIN, J.M., AND BRAGA, J.C., 1994, Messinian events in the Sorbas Basin in southeastern Spain and their implications in the recent history of the Mediterranean: Sedimentary geology, v. 90, p. 257-268.

MARTIN, J.M., BRAGA, J.C., AGUIRRE, J., AND BETZLER, C., 2004, Contrasting models of temperate carbonate sedimentation in a small Mediterranean embayment: the Pliocene Carboneras Basin, SE Spain: Journal of the Geological Society, London, v. 161, p. 387-399.

MARTIN, J.M., BRAGA, J.C., AND BETZLER, C., 2003, Late Neogene - Recent uplift of the Cabo de Gata volcanic province, Almeria, SE Spain: Geomorphology, v. 50, p. 27-42.

MARTIN, J.M., BRAGA, J.C., BETZLER, C., AND BRACHERT, T., 1996, Sedimentary model and high-frequency cyclicity in a Mediterranean, shallow-shelf, temperate-carbonate environment (uppermost Miocene, Agua Amarga Basin, Southern Spain): Sedimentology, v. 43, p. 263-277.

MCKIRAHAN, J.R., GOLDSTEIN, R.H., FRANSEEN, E.K., 2003, Build-and-Fill Sequences: How Subtle Paleotopography Affects 3-D Heterogeneity of Potential Reservoir Facies: SEPM Special Publication No. 78 and AAPG Memoir 83, p. 97-116.

MERCER, J.H., AND SUTTER, J.F., 1982, Late Miocene,-Earliest Pliocene Glaciation in Southern Argentina: Implications for Global Ice-sheet History: Palaeogeography, Palaeoclimatology, Palaeoecology, v. 38, p. 185-206.

MONTADERT, L., ROBERTS, D.G., AUFFRET, G.A., BOCK, W., DUPEUBLE, P.A., HAILWOOD, E.A., HARRISON, W., LETOUZEY, J., AND MAUFFRET, A., 1978, Messinian events: seismic evidence *in* Hsu, K.J., Montadert, L., Initial Reports of the Deep Sea Drilling: US Government Printing Office, Washington, v. 42, p. 1037-1050.

MONTENANT, C., AND OTT D'ESTEVOU, P. , 1990, Le basin de Nijar-Carboneras et le couloir de Bas-Andarax, *in* Montenant, C., ed., Les Bassins Neogenes Du Domaine Betique Oriental (Espagne): Institut Geologique Albert-de-Lapparent, Paris, Documents et Travaux Institut Geologique Albert-de-Lapparent, p. 129-164.

PLANAVSKY, N., AND GINSBURG, R.N., 2009, Taphonomy of Modern Marine Bahamian Microbialites: PALAIOS, v. 24, p. 5-17.

PLATT, J.P., AND VISSERS, R.L.M., 1989, Extensional collapse of thickened continental lithosphere: a working hypothesis for the Alboran sea and Gibraltar arc: Geology, v. 17, p. 540-543.

QI, L., AND CARR, T.R., 2003, Reservoir characterization of Mississippian St. Louis carbonate reservoir systems in Kansas: Stratigraphic and Facies Architecture Modeling: Annual Meeting Expanded Abstracts – American Association of Petroleum Geologists, v. 12, p. 141.

REHAULT, J.P., BOILLOT, G., AND MAUFFRET, A., 1985, The western Mediterranean basin, *in* Stanley, D.J., and Wezel, F.C., eds., Geologic Evolution of the Mediterranean Basin. Springer-Verlag, New York, p. 101-130.

READ, J.F., 1985, Carbonate platform facies models: AAPG Bulletin, v. 69, p. 1-21.

REID, R.P., JAMES, N.P., KINGSTON, I.G., MACINTYRE, I.G., DUPRAZ, C.P., AND BURNE, R.V., 2003, Shark Bay Stromatolites: Microfacies and Reinterpretation of Origins: Facies, v. 49, p. 45-53.

VALLES ROCA, D., 1986, Carbonate facies and depositional cycles in the upper Miocene of Santa Pola (Alicante, SE Spain): Revista d'Investigacions Geologiques, v. 42/43, p. 45-66.

ROUCHY, J.-M., AND SAINT MARTIN, J.-P., 1992, Late Miocene events in the Mediterranean as recorded by carbonate-evaporite relations: Geology, v. 20, p. 629-632.

RIDING, R., MARTIN, J.M., AND BRAGA, J.C., 1991, Coral-stromatolite reef framework, Upper Miocene, Almeria, Spain: Sedimentology, v. 38, p. 799-818.

SAMI, T.T., AND JAMES, N.P., 1994, Peritidal Carbonate Growth and Cyclicity in an Early Proterozoic Foreland Basin, Upper Pethei Group, Northwest Canada: Journal of Sedimentary Research, v. B64, p. 111-131.

SANZ DE GALDEANO, C. AND VERA, J.A., 1992, Stratigraphic record and palaeogeographical context of the Neogene basins in the Betic Cordilleran, Spain: Basins Research, v. 4, p. 21-36.

SERRANO, F., 1992, Biostratigraphic control of Neogene volcanism in Sierra De Gata (southeast Spain): Geologie en Mijnbouw, v. 71, p.3-14.

TOOMEY, N., 2003, Controls on sequence stratigraphy in upper Miocene carbonates of Cerro de Ricardillo, southeastern Spain [unpublished Unpublished M.S. thesis]: University of Kansas, Lawrence, KS, 114 p.

TUCKER, J.D., HITZMAN, D.C., AND ROUNTREE, B.A., 1997, Detailed Microbial Reservoir Characterization Identifies Reservoir Heterogeneities within a Mature Field in Oklahoma: Annual Meeting Expanded Abstracts – American Association of Petroleum Geologists, v. 81, p. 117.

TUCKER, M.E., AND WRIGHT, V.P., 1990, Carbonate Sedimentology: Oxford, Blackwell Scientific Publications, 482 p.

WHALEN, M.T., DAY, J., EBERLI, G.P., AND HOMEWOOD, P.W., 2002, Microbial carbonates as indicators of environmental change and biotic crises in carbonate systems: examples from the Late Devonian, Alberta basin, Canada: Palaeogeography, Palaeoclimatology, Palaeoecology, v. 181, p.127-151.

WHITESELL, T.C., 1995, Diagenetic Features Associated with Sequence Boundaries in Upper Miocene Carbonate Strata, Las Negras, Spain [unpublished Unpublished Master's Thesis]: University of Kansas, 292 p.

WRIGHT, V.P., AND BURCHETTE, T.P., 1996, Shallow-water carbonate environments, *in* Reading, H.G., ed., Sedimentary Environments: Processes, Facies, and Stratigraphy, 3rd edition, Oxford, England, Blackwell Science, p. 325-394.